

Oskarshamn site investigation

Interpretation of geophysical borehole measurements from KLX18A, KLX20A, KLX09B, KLX09D, KLX09F, KLX11B, HLX38, HLX39, HLX40, HLX41 and interpretation of petrophysical data from KLX20A

Håkan Mattsson, Mikael Keisu
GeoVista AB

December 2006

Svensk Kärnbränslehantering AB

Swedish Nuclear Fuel
and Waste Management Co
Box 5864

SE-102 40 Stockholm Sweden

Tel 08-459 84 00

+46 8 459 84 00

Fax 08-661 57 19

+46 8 661 57 19



Oskarshamn site investigation

Interpretation of geophysical borehole measurements from KLX18A, KLX20A, KLX09B, KLX09D, KLX09F, KLX11B, HLX38, HLX39, HLX40, HLX41 and interpretation of petrophysical data from KLX20A

Håkan Mattsson, Mikael Keisu

GeoVista AB

December 2006

Keywords: Borehole, Logging, Geophysics, Geology, Bedrock, Fractures.

This report concerns a study which was conducted for SKB. The conclusions and viewpoints presented in the report are those of the authors and do not necessarily coincide with those of the client.

A pdf version of this document can be downloaded from www.skb.se

Abstract

This report presents the compilation and interpretation of geophysical logging data from the cored boreholes KLX18A, KLX20A, KLX09B, KLX09D, KLX09F, KLX11B and the percussion drilled boreholes HLX38, HLX39, HLX40 and HLX41. The report also includes the interpretation of petrophysical data from KLX20A.

The main objective of the investigation is to use the results as supportive information during the geological core logging and mapping of drill cuttings and as supportive information during the geological single-hole interpretation.

The cored boreholes KLX20A and KLX11B are dominated by rocks with silicate density in the range 2,730–2,800 kg/m³, natural gamma radiation of 10–20 µR/h and magnetic susceptibility of 0.025–0.030 SI. The combination of physical parameters is typical for quartz monzodiorite rock. In KLX20A the occurrence of highly fractured dolerite rock is indicated by both logging and petrophysical data in the section c 182–231 m. In the lower half of KLX11B the occurrences of three possible deformation zones are indicated.

The other four cored boreholes (KLX18A, KLX09B, D and F) have silicate density mainly < 2,680 kg/m³ and 2,680–2,730 kg/m³. The natural gamma radiation is generally in the interval 10–30 µR/h and the magnetic susceptibility is in the range c 0.015–0.040 SI. This combination of physical parameters is typical for Ävrö granite. The silicate density data reveal clear patterns of compositional variations of the Ävrö granite in all four boreholes. A few possible deformation zones are identified in KLX09B, D and F, but the fracture frequency in these boreholes is mainly low or partly moderate. The fracture frequency estimated for KLX18A shows large variations, with several sections of increased fracturing. Possible deformation zones are indicated in the sections c 138–150 m, 284–300 m, 398–406 m, 448–451 m and 484–488 m. Decreased P-wave velocity, generally related to strong brittle fracturing, occurs within the sections 284–300 m, 398–406 m and 484–488 m.

The four percussion drilled boreholes generally show silicate density < 2,680 kg/m³ and 2,680–2,730 kg/m³. The natural gamma radiation is mainly in the interval 10–20 µR/h and the magnetic susceptibility is in the range c 0.015–0.030 SI. In HLX38 there is a clear dominance of density in the range 2,680–2,730 kg/m³ and in HLX41 there is a dominance of density < 2,680 kg/m³. The data most likely indicate a dominant occurrence of Ävrö granite in the vicinity of the all four boreholes, however with mainly granodioritic mineral composition in HLX38 and dominant granitic composition in HLX41. In HLX39 and HLX40 the compositional variations appear to be more mixed.

The estimated fracture frequency is mainly low, partly moderate, in the percussion drilled boreholes, but few minor deformation zones occur in certain places. In HLX38 there is a major decrease in magnetic susceptibility in the section c 74–101 m, which may indicate mineral alteration. There are no density data available in the section so the reason for the low susceptibility is difficult to explain. Resistivity and sonic data only indicate partly increased fracturing.

Sammanfattning

Föreliggande rapport presenterar en sammanställning och tolkning av geofysiska borrhålsmätningar från kärnborrhålen KLX18A, KLX20A, KLX09B, KLX09D, KLX09F, KLX11B och de hammarborrhålen HLX38, HLX39, HLX40 samt HLX41. Rapporten behandlar även tolkning av petrofysiska data från KLX20A.

Huvudsyftet med undersökningen är att ta fram ett material som på ett förenklat sätt åskådliggör resultaten av de geofysiska loggningarna, s k generaliserade geofysiska loggar. Materialet används dels som stödjande data vid borrhärne- och borrhärkaxkarteringen samt som underlag vid den geologiska enhålstolkningen.

Kärnborrhålen KLX20A och KLX11B domineras av bergarter med silikatdensitet i intervallet 2,730–2,800 kg/m³, naturlig gammastrålning i intervallet 10–20 µR/h och magnetisk susceptibilitet i intervallet 0,025–0,030 SI. Kombinationen av fysikaliska egenskaper är typisk för kvartsmonzodiorit. I KLX20A indikerar loggdata och petrofysiska data tillsammans förekomst av en kraftigt uppsprucken diabas längs ca 182–231 m. I den nedre halvan av KLX11B har tre möjliga deformationszoner identifierats.

I de övriga fyra kärnborrhålen, KLX18A, KLX09B, D och F, förekommer silikatdensitet främst i intervallen < 2,680 kg/m³ och 2,680–2,730 kg/m³. Naturlig gammastrålning är 10–30 µR/h och den magnetiska susceptibiliteten är ca 0,015–0,040 SI. Denna kombination av fysikaliska egenskaper är typisk för Ävrögranit. Silikatdensitetloggarna påvisar tydliga variationer i mineralsammansättning för Ävrögraniten i de fyra borrhålen. Enstaka möjliga deformationszoner förekommer i KLX09B, D och F, men den uppskattade sprickfrekvensen är generellt låg i dessa borrhål. I KLX18A uppvisar den uppskattade sprickfrekvensen stora variationer, och det förekommer flera avsnitt med förhöjd sprickfrekvens. Möjliga deformationszoner kan identifieras längs sektionerna ca 138–150 m, 284–300 m, 398–406 m, 448–451 m och 484–488 m. Kraftig spröd deformation, indikerad bl.a. av sänkt P-vågshastighet, förekommer inom sektionerna 284–300 m, 398–406 m, och 484–488 m.

De fyra hammarborrhålen domineras av silikatdensitet i intervallen < 2,680 kg/m³ och 2,680–2,730 kg/m³. Naturlig gammastrålning är 10–20 µR/h och den magnetiska susceptibiliteten är ca 0,015–0,030 SI. I HLX38 är silikatdensiteten främst i intervallet 2,680–2,730 kg/m³ och i HLX41 är silikatdensiteten generellt < 2,680 kg/m³. Loggdata indikerar dominerande förekomst av Ävrögranit i samtliga fyra borrhål, men i HLX38 har bergarten granodioritisk mineralsammansättning och i HLX41 dominerar granitisk mineralsammansättning. I HLX39 och HLX40 verkar fördelning av mineralsammansättning vara mer spridd.

Den uppskattade sprickfrekvensen är generellt låg, ibland något förhöjd, i samtliga fyra hammarborrhålen. Enstaka mindre deformationszoner förekommer dock. I HLX38 är susceptibiliteten kraftigt sänkt längs intervallet ca 74–101 m, vilket kan tyda på mineralomvandling. Längs sektionen saknas dock densitetsdata vilket försvårar möjligheten att förklarar den låga susceptibiliteten. Resistivitetloggarna och sonic-loggen indikerar endast mindre avsnitt med förhöjd sprickfrekvens i detta område.

Contents

1	Introduction	7
2	Objective and scope	9
3	Equipment	11
3.1	Description of equipment for analyses of logging data	11
3.2	Description of equipment for analyses of petrophysical data	11
4	Execution	13
4.1	Laboratory measurements	13
4.2	Interpretation of the logging data	14
4.3	Preparations and data handling	16
4.4	Analyses and interpretations	16
4.5	Nonconformities	16
5	Results	17
5.1	Petrophysical properties of KLX20A	17
5.2	Quality control of the logging data	18
5.3	Interpretation of the logging data	20
5.3.1	Interpretation of KLX18A	20
5.3.2	Interpretation of KLX20A	22
5.3.3	Interpretation of KLX09B	25
5.3.4	Interpretation of KLX09D	28
5.3.5	Interpretation of KLX09F	32
5.3.6	Interpretation of KLX11B	35
5.3.7	Interpretation of HLX38	35
5.3.8	Interpretation of HLX39	39
5.3.9	Interpretation of HLX40	39
5.3.10	Interpretation of HLX41	42
	References	45
Appendix 1	Generalized geophysical logs of KLX18A	47
Appendix 2	Generalized geophysical logs of KLX20A	49

1 Introduction

SKB performs site investigations for localization of a deep repository for high level radioactive waste. The site investigations are performed at two sites, Forsmark and Oskarshamn. This document reports the results gained from the interpretation of geophysical borehole logging data from the cored boreholes KLX18A, KLX20A, KLX09B, KLX09D, KLX09F, KLX11B and the percussion drilled boreholes HLX38, HLX39, HLX40 and HLX41, located in Laxemar, Oskarshamn. The report also includes the interpretation of petrophysical data from KLX20A.

Generalized geophysical loggings related to lithological variations are presented together with indicated fracture loggings, including estimated fracture frequency. Calculations of the salinity are also presented. The logging measurements were conducted in 2006 by Rambøll /1/.

The interpretation presented in this report is performed by GeoVista AB in accordance with the instructions and guidelines from SKB (activity plan AP PS 400-06-074 and method descriptions MD 221.003, MD 230.001 and MD 160.002, SKB internal controlling documents), Table 1-1.

Figure 1-1 shows the location of boreholes KLX18A, KLX20A, KLX09B, KLX09D, KLX09F, KLX11B, HLX38, HLX39, HLX40 and HLX41.

The interpreted results are stored in the primary data base SICADA and are traceable by the activity plan number.

Table 1-1. Controlling documents for the performance of the activity

Activity plan	Number	Version
Tolkning av borrhålsgeofysiska data från KLX20A, KLX18A, KLX11B, KLX09B, KLX09D, KLX09F samt HLX38, HLX39, HLX40 och HLX41	AP PS 400-06-074	1.0
Method descriptions	Number	Version
Metodbeskrivning för bestämning av densiteten och porositeten hos det intakta berget	SKB MD 160.002	2.0
Metodbeskrivning för mätning av bergarters petrofysiska egenskaper	SKB MD 230.001	2.0
Metodbeskrivning för tolkning av geofysiska borrhålsdata	SKB MD 221.003	2.0

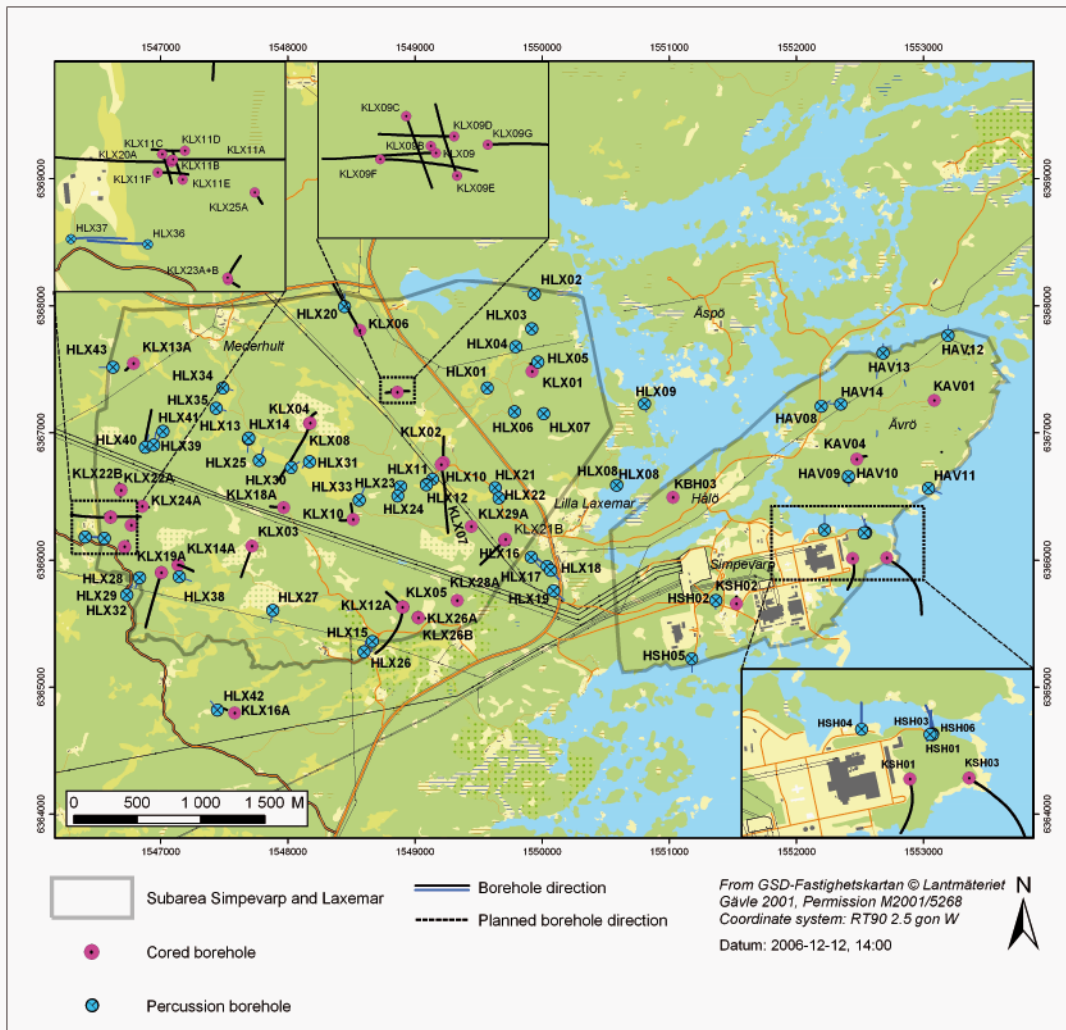


Figure 1-1. Location of the boreholes KLX18A, KLX20A, KLX09B, KLX09D, KLX09F, KLX11B, HLX38, HLX39, HLX40 and HLX41 in Laxemar.

2 Objective and scope

The purpose of geophysical measurements in boreholes is to gain knowledge of the physical properties of the bedrock in the vicinity of the borehole. A combined interpretation of the “lithological” logging data; silicate density, magnetic susceptibility and natural gamma radiation, together with petrophysical data makes it possible to estimate the physical signature of different rock types. The three loggings are generalized and are then presented in a simplified way. The location of major fractures and an estimation of the fracture frequency along the borehole are calculated by interpreting data from the resistivity loggings; the single point resistance (SPR), caliper and sonic loggings.

An estimation of the salinity and the apparent porosity are presented for the borehole. These parameters indicate salinity variations in the borehole fluid and the transport properties of the rock volume in the vicinity of the borehole.

The petrophysical measurements give information of the physical characteristics of rocks, which supports the rock type classification and allows calibration of geophysical logs.

The main objective of these investigations is to use the results as supportive information during the geological core logging and as supportive information during the so called “geological single-hole interpretation”, which is a combined borehole interpretation of core logging (Boremap) data, geophysical data and radar data.

3 Equipment

3.1 Description of equipment for analyses of logging data

The software used for the interpretation are WellCad v4.0 (ALT) and Strater 1.00.24 (Golden Software), that are mainly used for plotting, Grapher v5 (Golden Software), mainly used for plotting and some statistical analyses, and a number of in-house software developed by GeoVista AB on behalf of SKB.

3.2 Description of equipment for analyses of petrophysical data

The measurements of magnetic susceptibility were performed with a KLY-3 Kappabridge from Geofyzika Brno. The natural remanent magnetization (NRM) was measured with a SQUID magnetometer from 2G Enterprises. Masses for the density determinations were measured with a digital Mettler Toledo PG 5002. The measurements were performed by the petrophysical laboratory at Luleå University of Technology.

4 Execution

4.1 Laboratory measurements

The sampling covers 11 samples from KLX20A (Table 4-1), collected and preliminary classified by SKB. Preparations of the drill cores were performed by a technician at the laboratory of the Division of Applied Geophysics, Luleå University of Technology. The measurements of the magnetic susceptibility and NRM were performed according to MD 230.001 (SKB internal controlling document). The measurements of the wet density were performed according to MD 160.002 (SKB internal controlling document). The instruction is written to conform to rock mechanical measurements on drill cores from deep drillings, where the density determinations are parts of other types of measurements, not directly relevant for the geological core logging. The time to soak the samples (48 hours in this investigation) is e.g. shorter than what is recommended in MD 160.002.

Calibration of instruments for measurements of petrophysical parameters were performed in accordance to the manual for each instrument respectively.

The laboratory measurements of petrophysical parameters produce raw-data files in ascii, binary or Microsoft Excel formats. All data files were delivered via email from the laboratory at the Luleå University of Technology to GeoVista AB. The data were then rearranged and placed in Microsoft Excel files. Back-up files of all raw-data are stored both at GeoVista AB and at the laboratory.

Sample information, section up and section low, for KLX20A is given in Table 4-1.

Table 4-1. Sample information for KLX20A.

Section up (m)	Section low (m)	Rock type (preliminary classification)
159.91	160.03	Quartz monzodiorite
171.8	171.50	Quartz monzodiorite
181.97	182.09	Quartz monzodiorite
182.54	182.66	Dolerite
188.85	188.97	Dolerite
193.18	193.30	Dolerite
214.25	214.37	Dolerite
226.50	226.62	Dolerite
231.72	231.84	Quartz monzodiorite
237.77	237.89	Quartz monzodiorite
245.65	245.77	Quartz monzodiorite

4.2 Interpretation of the logging data

The execution of the interpretation can be summarized in the following five steps:

1. Preparations of the logging data (calculations of noise levels, filtering, error estimations, re-sampling, drift correction, length adjustment).

The loggings are median or mean filtered (generally 5 point filters for the resistivity loggings and 3 point filters for other loggings) and re-sampled to common section coordinates (0.1 m point distance).

The density (logging tool century 9139) and magnetic susceptibility logging data are calibrated with respect to petrophysical data. The magnetic susceptibility logging data were calibrated by use of a combination of petrophysical data from the boreholes KLX03, KSH01A, KSH02, KSH03A, KAV04A and KLX10 see /2, 3, 4, 5, 6, 7/. The density logging data were calibrated by use of petrophysical data from the borehole KLX20A (presented in this report).

The caliper 1D and caliper 3D logs are calibrated by use of borehole technical information supplied by SKB. The calibration procedure is described in detail in /8/.

2. Interpretation of rock types (generalization of the silicate density, magnetic susceptibility and natural gamma radiation loggings).

The silicate density is calculated with reference to /9/ and the data are then divided into 5 sections indicating a mineral composition corresponding to granite, granodiorite, tonalite, diorite and gabbro rocks, according to /10/. The sections are bounded by the threshold values

granite < 2,680 kg/m³
2,680 kg/m³ < granodiorite < 2,730 kg/m³
2,730 kg/m³ < tonalite < 2,800 kg/m³
2,800 kg/m³ < diorite < 2,890 kg/m³
2,890 kg/m³ < gabbro

The magnetic susceptibility logging is subdivided into steps of decades and the natural gamma radiation is divided into steps of "low" (< 10µR/h), "medium" (10 µR/h < gamma < 20 µR/h), "high" (20 µR/h < gamma < 30 µR/h) and "very high" (> 30 µR/h).

3. For the cored borehole the normal resistivity loggings are corrected for the influence of the borehole diameter and the borehole fluid resistivity. The apparent porosity is calculated during the correction of the resistivity loggings. The calculation is based on Archie's law /11/; $\sigma = a \sigma_w \phi^m + \sigma_s$ where σ = bulk conductivity (S/m), σ_w = pore water conductivity (S/m), ϕ = volume fraction of pore space, σ_s = surface conductivity (S/m) and "a" and "m" are constants. Since "a" and "m" vary significantly with variations in the borehole fluid resistivity, estimations of the constants are performed with reference to the actual fluid resistivity in each borehole respectively.
4. Interpretation of the position of large fractures and estimated fracture frequency (classification to fracture logging and calculation of the estimated fracture frequency logging are based on analyses of the short and long normal resistivity, caliper mean, single point resistance (SPR), focused resistivity (140 and 300 cm) and sonic).

The position of large fractures is estimated by applying a second derivative filter to the logging data and then locating maxima (or minima depending on the logging method) in the filtered logging. Maxima (or minima) above (below) a certain threshold value (Table 4-2) are selected as probable fractures. The result is presented as a column diagram where column

height 0 = no fracture, column height 1 = fracture indicated by all logging methods. The estimated fracture frequency is calculated by applying a power function to the weighted sum of the maxima (minima) derivative logging for each method respectively, and then calculating the total sum of all power functions. Parameters for the power functions were estimated by correlating the total weighted sum to the mapped fracture frequency in the cored boreholes KLX03 and KLX04 /2/. The powers and linear coefficients (weights) used are presented in Table 4-2.

5. Report evaluating the results.

Table 4-2. Threshold values, powers and weights used for estimating position of fractures and calculate estimated fracture frequency, respectively.

	Borehole	Sonic	Focused res. 140	Focused res. 300	Caliper	SPR	Normal res. 64	Normal res. 16	Lateral res.
Threshold	KLX18A	2.0	3.0	2.0	1.0	3.0	-----	7.0	-----
Power	KLX18A	1.0	1.0	1.6	1.0	0.5	0.5	0.6	-----
Weight	KLX18A	1.0	7.1	6.7	1.0	5.0	2.9	5.0	-----
Threshold	KLX20A	2.0	3.0	1.5	1.0	1.7	1.3	7.0	-----
Power	KLX20A	1.0	1.0	1.6	1.0	0.5	0.5	0.6	-----
Weight	KLX20A	1.0	7.1	6.7	1.0	5.0	2.9	5.0	-----
Threshold	KLX09B	2.0	1.2	1.0	1.0	1.0	5.0	5.0	-----
Power	KLX09B	1.0	1.0	1.6	1.0	0.5	0.5	0.6	-----
Weight	KLX09B	1.0	7.1	6.7	1.0	5.0	2.9	5.0	-----
Threshold	KLX09D	1.0	1.2	1.5	0.5	1.0	4.0	4.0	-----
Power	KLX09D	1.0	1.0	1.6	1.0	0.5	0.5	0.6	-----
Weight	KLX09D	1.0	7.1	6.7	1.0	5.0	2.9	5.0	-----
Threshold	KLX09F	1.0	1.5	1.5	0.5	1.0	5.0	5.0	-----
Power	KLX09F	1.0	1.0	1.6	1.0	0.5	0.5	0.6	-----
Weight	KLX09F	1.0	7.1	6.7	1.0	5.0	2.9	5.0	-----
Threshold	KLX11B	1.5	1.5	1.0	0.5	1.0	5.0	4.0	-----
Power	KLX11B	1.0	1.0	1.6	1.0	0.5	0.5	0.6	-----
Weight	KLX11B	1.0	7.1	6.7	1.0	5.0	2.9	5.0	-----
Threshold	HLX38	1.5	1.5	1.5	0.5	1.0	5.0	4.0	-----
Power	HLX38	1.0	1.0	1.6	1.0	0.5	0.5	0.6	-----
Weight	HLX38	1.0	7.1	6.7	1.0	5.0	2.9	5.0	-----
Threshold	HLX39	1.5	1.5	1.5	0.6	1.0	5.0	4.0	-----
Power	HLX39	1.0	1.0	1.6	1.0	0.5	0.5	0.6	-----
Weight	HLX39	1.0	7.1	6.7	1.0	5.0	2.9	5.0	-----
Threshold	HLX40	1.5	1.5	1.5	0.5	1.0	4.0	4.0	-----
Power	HLX40	1.0	1.0	1.6	1.0	0.5	0.5	0.6	-----
Weight	HLX40	1.0	7.1	6.7	1.0	5.0	2.9	5.0	-----
Threshold	HLX41	1.5	1.5	1.5	0.5	1.7	7.0	5.0	-----
Power	HLX41	1.0	1.0	1.6	1.0	0.5	0.5	0.6	-----
Weight	HLX41	1.0	7.1	6.7	1.0	5.0	2.9	5.0	-----

4.3 Preparations and data handling

The logging data were delivered as Microsoft Excel files via email from SKB. The data of each logging method is saved separately as an ASCII-file. The data processing is performed on the ASCII-files. The data used for interpretation are:

- Density (gamma-gamma)
- Magnetic susceptibility
- Natural gamma radiation
- Focused resistivity (300 cm)
- Focused resistivity (140 cm)
- Sonic (P-wave)
- Caliper mean
- Caliper 1D
- SPR
- Fluid resistivity
- Fluid temperature

The borehole technical information used for calibration of the caliper data is delivered as Microsoft Word files via email by SKB.

4.4 Analyses and interpretations

The analyses of the logging data are made with respect to identifying major variations in physical properties with depth as indicated by the silicate density, the natural gamma radiation and the magnetic susceptibility. Since these properties are related to the mineral composition of the rocks in the vicinity of the borehole they correspond to variations in lithology and in thermal properties.

The resistivity, sonic and caliper loggings are mainly used for identifying sections with increased fracturing and alteration. The interpretation products salinity and apparent porosity help identifying saline ground water and porous rocks.

4.5 Nonconformities

In some boreholes the long normal resistivity logging measurements show unrealistic anomalies. Apparent porosity calculations and corrections for the borehole diameter and fluid resistivity are therefore only presented for the short normal resistivity data. Apart from this, no nonconformities are reported.

5 Results

5.1 Petrophysical properties of KLX20A

The rock type classifications diagram in Figure 5-1 shows the distribution of the magnetic susceptibility versus density for the 11 core samples (see also Table 4-1).

The petrophysical data indicate that the dolerite has an average density of $2,893 \pm 20 \text{ kg/m}^3$ (when excluding the outlying sample from the contact zone at c 182.6 m). The mean susceptibility of the dolerite is 0.011 SI, which is only slightly lower than the mean susceptibility of the surrounding quartz monzodiorite of 0.022 SI. The quartz monzodiorite samples show a large scatter in density, averaging at $2,745 \pm 43 \text{ kg/m}^3$. The sample with lowest density is collected close to the boundary between the quartz monzodiorite and the dolerite (182.0 m), and this density value is most likely affected by fracturing.

The petrophysical data of the dolerite suggest that the rock is fairly fresh and have not suffered from any significant alteration (possibly only weak alteration). Strong alteration would most likely have resulted in destruction of magnetite (decreased magnetic susceptibility) and also decreased density. In Figure 5-1 it is clearly indicated that the dolerite carries ferromagnetic minerals, most likely magnetite.

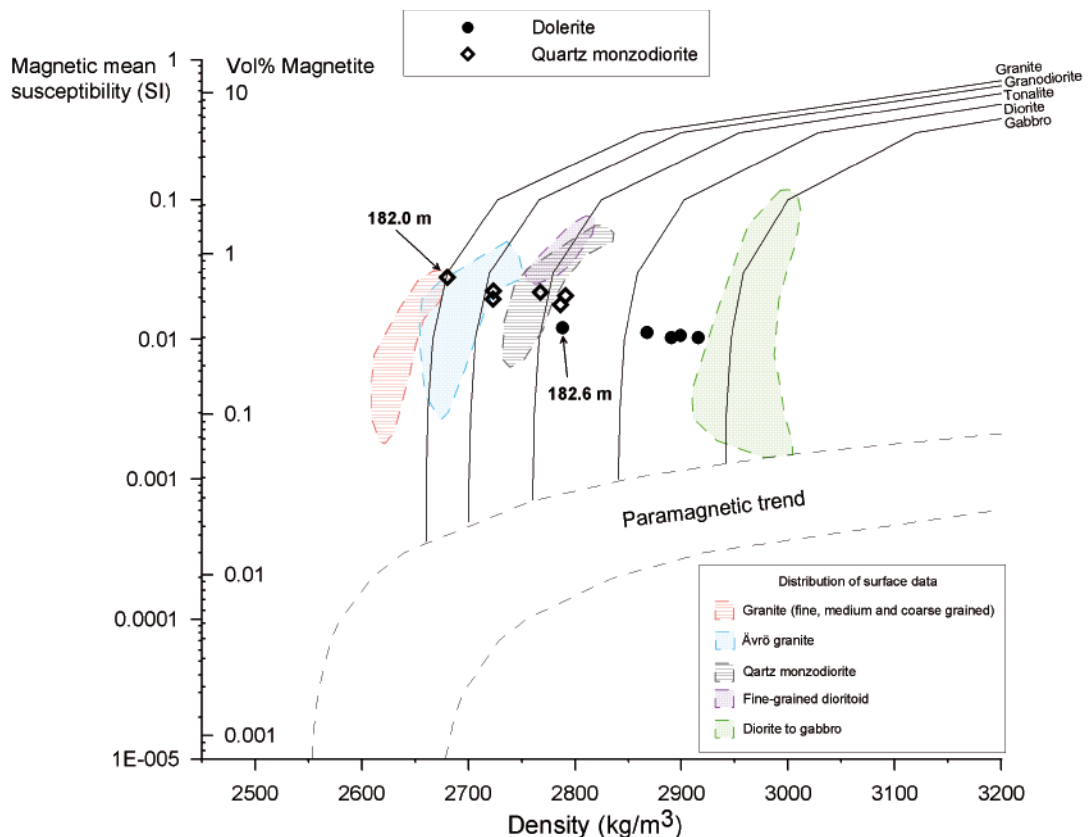


Figure 5-1. Susceptibility – density rock classification diagram. The shaded areas indicate the distribution of some of the rock types group from the collection of samples on the surface in the Laxemar and Simpevarp area. The two arrows indicate samples collected close to the upper contact of the dolerite.

This interpretation is also supported by the NRM data (Figure 5-2). The mean natural remanent magnetisation of the dolerite is 174 ± 93 mA/m and the Q-values are in the range $Q = 0.37 - 0.61$. As reference, fresh post-jotnian dolerites have mean susceptibility of c 0.02–0.04 SI and NRM of 1,000–2,000 mA/m.

5.2 Quality control of the logging data

Noise levels of the raw data for each logging method are presented in Table 5-1. The density, natural gamma radiation and magnetic susceptibility logging data are above the recommended noise levels for all the investigated boreholes. The boreholes KLX20A, KLX09B, KLX09D, KLX11B and HLX41 have significantly increased noise levels in the density data and in KLX09B, KLX09D, KLX09F, KLX11B, HLX39 and HLX41 the noise of the natural gamma radiation data are greatly increased. To reduce the influence from the noise all data were average filtered prior to the evaluation.

A qualitative inspection was performed on the loggings. The data were checked for spikes and/or other obvious incorrect data points. Erroneous data were replaced by null values (-999) by the contractor Rambøll prior to the delivery of the data, and all null values were disregarded in the interpretation. Sections with null values are indicated by red and white stripes in the presentation of the generalized loggings. In HLX38 the entire section c 64–125 m lacks density and caliper data.

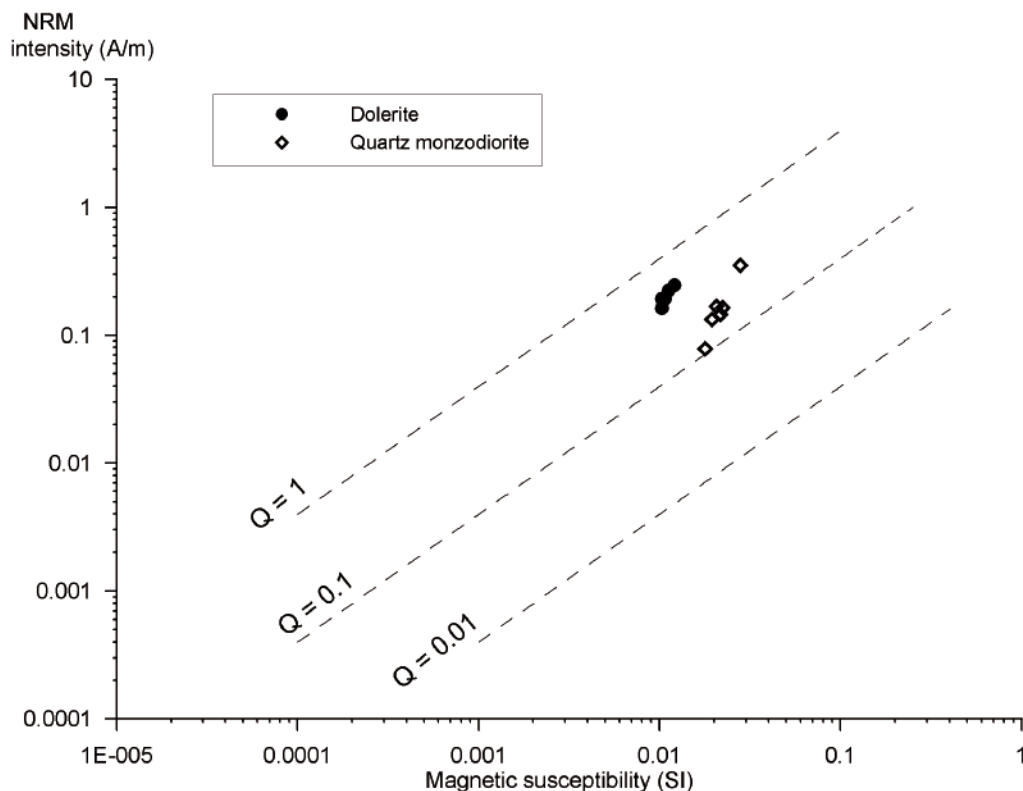


Figure 5-2. Susceptibility – NRM (Natural Remanent Magnetiation) diagram.

Table 5-1. Noise levels in the investigated geophysical logging data.

Logging method	KLX18A	KLX20A	KLX09B	KLX09D	KLX09F	KLX11B	HLX38	HLX39	HLX40	HLX41	Recommended max noise level
Density (kg/m ³)	12	18	18	18	12	19	12	11	10	17	3 – 5
Magnetic susceptibility (SI)	4·10 ⁻⁴	3·10 ⁻⁴	6·10 ⁻⁴	6·10 ⁻⁴	4·10 ⁻⁴	3·10 ⁻⁴	2·10 ⁻⁴	4·10 ⁻⁴	5·10 ⁻⁴	5·10 ⁻⁴	1·10 ⁻⁴
Natural gamma radiation (µR/h)	0.7	0.6	1.5	1.4	1.6	1.4	0.6	1.2	0.3	1.1	0.3
Long normal resistivity (%)	Not used	0.5	0.7	2.8	1.3	0.9	0.9	0.2	0.1	1.0	2.0
Short normal resistivity (%)	0.2	0.2	0.5	3.0	1.3	0.5	0.2	0.1	0.1	0.8	2.0
Fluid resistivity (%)	0.009	0.02	0.008	0.01	0.1	0.05	0.03	0.02	0.04	0.02	2
Fluid temperature (°C)	0.3·10 ⁻³	0.3·10 ⁻³	0.4·10 ⁻³	0.4·10 ⁻³	0.9·10 ⁻³	8·10 ⁻³	7·10 ⁻⁴	1·10 ⁻³	0.01	7·10 ⁻⁴	0.01
Lateral resistivity (%)	Not used	Not used	Not used	Not used	No used	Not used	Not used	Not used	Not used	Not used	2
Single point resistance (%)	0.2	0.2	0.3	0.5	0.4	0.6	0.4	0.1	0.1	0.3	No data
Caliper 1D	0.1·10 ⁻⁵	0.2·10 ⁻⁵	0.5·10 ⁻⁵	0.4·10 ⁻⁵	0.3·10 ⁻⁵	0.3·10 ⁻⁵	4·10 ⁻⁵	7·10 ⁻⁵	4·10 ⁻⁵	1·10 ⁻⁴	5·10 ⁻⁴
Caliper mean (m)	1·10 ⁻⁵	3·10 ⁻⁵	No data	No data	No data	0.2·10 ⁻⁴	No data	No data	No data	No data	5·10 ⁻⁴
Focused resistivity 300 (%)	9.2	12.8	10.1	16.6	13.7	18.2	9.9	6.9	8.1	10.4	No data
Focused resistivity 140 (%)	1.7	2.9	2.5	12.0	4.1	3.2	2.4	4.6	1.5	2.2	No data
Sonic (m/s)	1	2	15	19	16	6	9	5	7	11	20

5.3 Interpretation of the logging data

The presentation of interpretation products presented below includes:

- Classification of silicate density.
- Classification of natural gamma radiation.
- Classification of magnetic susceptibility.
- Position of inferred fractures (0 = no method, 1 = all methods).
- Estimated fracture frequency in 5 metre sections.
- Classification of estimated fracture frequency (0 to 3, 3 to 6 and > 6 fractures/m).

5.3.1 Interpretation of KLX18A

The results of the generalized logging data and fracture estimations of KLX18A are presented in Figure 5-3 and in a more detailed scale in Appendix 1. The distribution of silicate density classes along the borehole is presented in Table 5-2.

Based on the silicate density log KLX18A can roughly be divided in two halves, section c 100–336 m and c 336–609 m. The upper half is dominated by silicate density in the interval 2,680–2,730 kg/m³, and slightly higher densities. The lower half is dominated by silicate density < 2,680 kg/m³, however with a few sections with density in the interval 2,680–2,730 kg/m³ at c 440–450 m, 486–506 m and 591–603 m.

The division of the borehole is also clearly indicated by the natural gamma radiation (Figure 5-3). In the section c 100–322 m the natural gamma radiation is mainly in the range 10–15 µR/h and in the section 322–607 m the natural gamma radiation is mainly in the range 18–25 µR/h. The magnetic susceptibility of the upper section averages at c 0.04 SI whereas in the lower section it averages at c 0.03 SI, which is a small but significant difference.

The physical property differences between the two halves suggest the occurrence of two different main rock types in KLX18A, or possibly that the borehole intersects two types of Ävrö granite with significant compositional variations. The upper half may be dominated by Ävrö granite with granodioritic composition and the lower half of Ävrö granite with granitic composition.

Rocks with density above 2,880 kg/m³ occur in the intervals c 196–206 m, 293–296 m, 332–334 m, 580–582 m and 603–607 m. The intervals coincide with decreased natural gamma radiation and decreased magnetic susceptibility, which suggests that the anomalies indicate the occurrences of mafic rocks, most likely fine grained diorite/gabbro. The uppermost section (196–206 m) is spatially related with intervals of increased natural gamma radiation, most likely related to fine grained granite, which indicates the occurrence of composite dykes.

Table 5-2. Distribution of silicate density classes with borehole length of KLX18A.

Silicate density interval (kg/m ³)	Borehole length (m)	Relative borehole length (%)
dens < 2,680	194	38
2,680 < dens < 2,730	220	43
2,730 < dens < 2,800	75	15
2,800 < dens < 2,890	9	2
dens > 2,890	8	2

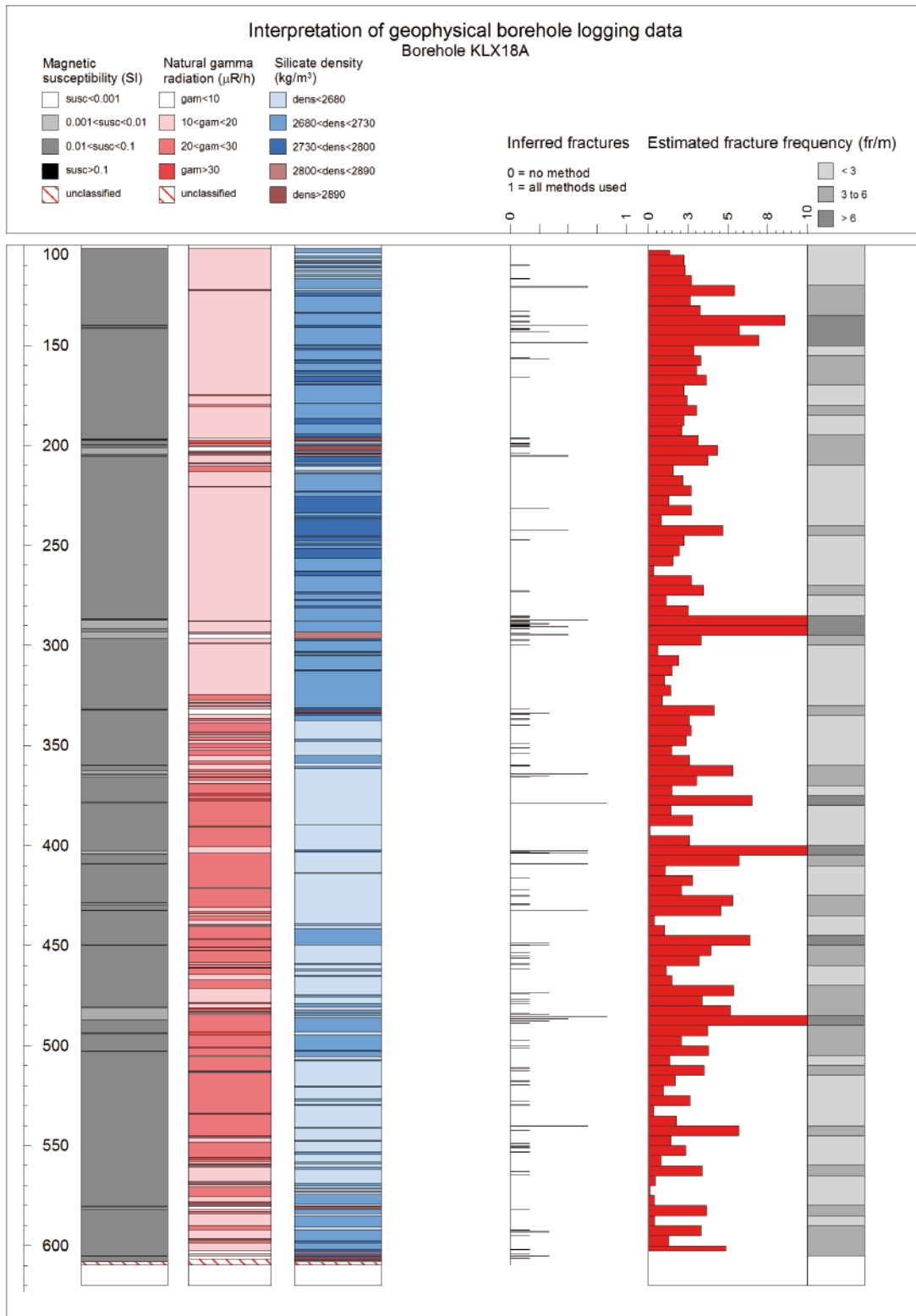


Figure 5-3. Generalized geophysical logs of KLX18A.

There are very few indications of fine-grained granite dykes in KLX18A. Apart from the anomalies at 196–206 m there are 4 intervals, less than 1 m long, in the section 480–560 m.

The fracture frequency estimated for KLX18A shows large variations, with several sections of increased fracturing. Possible deformation zones are indicated in the sections c 138–150 m, 284–300 m, 398–406 m, 448–451 m and 484–488 m. These intervals are all characterized by major decrease in the resistivity and magnetic susceptibility. Decreased P-wave velocity, generally related to strong brittle fracturing, occurs within the sections 284–300 m, 398–406 m and 484–488 m. In the interval 398–406 m there is a significant caliper anomaly. Major caliper anomalies also occur in the interval c 196–206 m, which coincides with the composite dykes suggested above.

The estimated apparent porosity (Figure 5-4) averages at c 0.5%, which is considered normal for crystalline rocks in this area. Increased porosity is clearly related to possible deformation zones, and mainly occurs in the section c 400–500 m. The estimated fluid water salinity averages at c 260 ppm NaCl in the section c 100–480 m. At c 480 m there is a large increase in salinity (possibly related to the indicated deformation zone), and the increase continues to the end of the borehole with a final salinity level of c 2,630 ppm NaCl.

5.3.2 Interpretation of KLX20A

The results of the generalized logging data and fracture estimations of KLX20A are presented in Figure 5-5 and in a more detailed scale in Appendix 2. The distribution of silicate density classes along the borehole is presented in Table 5-3.

The rocks in the vicinity of KLX20A are dominated by silicate density in the interval 2,730–2,800 kg/m³, in combination with rocks with silicate density in the interval 2,680–2,730 kg/m³ (Table 5-3). Along these sections the magnetic susceptibility is fairly constant within the interval c 0.025–0.030 SI and the natural gamma radiation is also fairly constant in the range 15–20 µR/h. The combination of physical properties most likely indicates a dominant occurrence of quartz monzodiorite, possibly in combination with Ävrö granite with high content of dark minerals and/or low content of quartz.

The section c 182–231 m is characterized by density in the range 2,820–2,920 kg/m³, natural gamma radiation in the range 4–5 µR/h and the magnetic susceptibility is fairly constant within the interval c 0.009–0.012 SI. The inspection of the core samples in combination with the physical properties shows that the rock is classified as dolerite.

In the section 393–401 m the density and natural gamma radiation data remind a great deal of those along the dolerite. However, the magnetic susceptibility is strongly decreased, in the range 0.0017–0.0027 SI, which suggests the occurrence of fine-grained diorite/gabbro.

There is a fair occurrence of strong positive natural gamma radiation anomalies along the entire borehole length. The anomalies are generally less than one meter long and most likely correspond to minor fine-grained granite dykes.

Table 5-3. Distribution of silicate density classes with borehole length of KLX20A.

Silicate density interval (kg/m ³)	Borehole length (m)	Relative borehole length (%)
dens < 2,680	10	3
2,680 < dens < 2,730	77	22
2,730 < dens < 2,800	225	63
2,800 < dens < 2,890	31	9
dens > 2,890	11	3

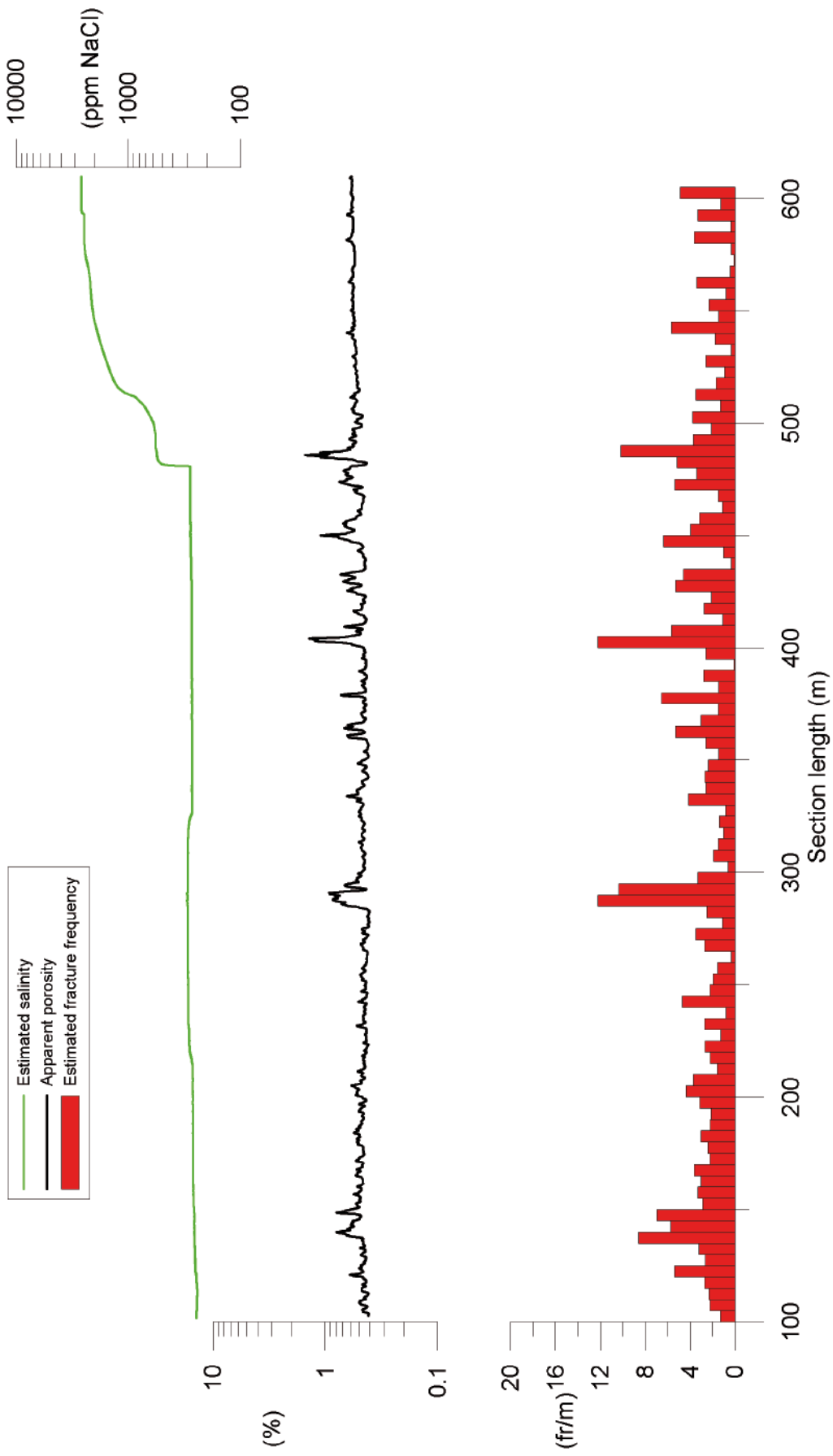


Figure 5-4. Estimated salinity, apparent porosity and estimated fracture frequency of KLX18A.

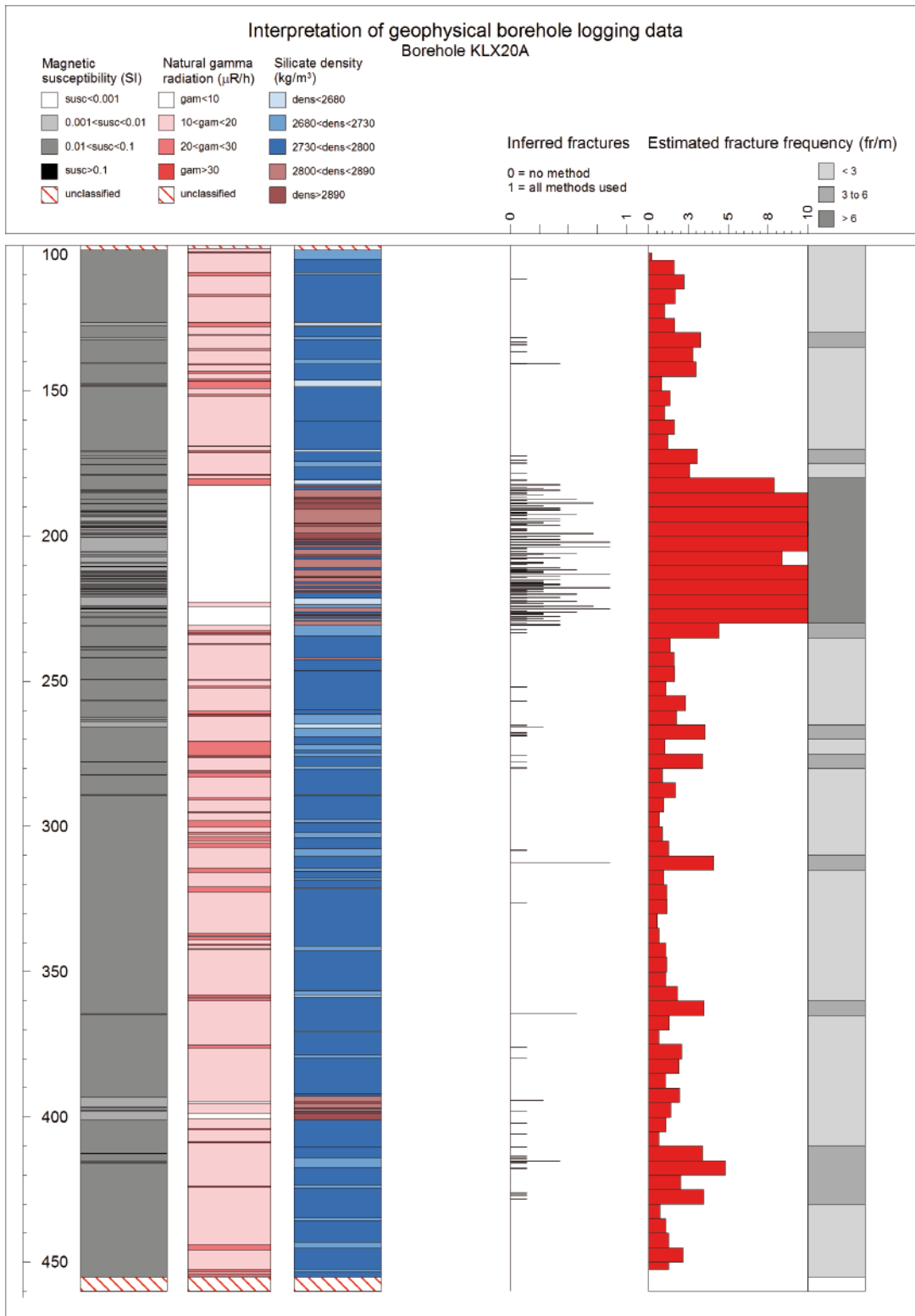


Figure 5-5. Generalized geophysical logs of KLX20A.

The dolerite at c 182–231 m is characterized by a major decrease in electric resistivity, decreased P-wave velocity and several strong caliper anomalies, which clearly indicates that this rock is heavily fractured. The host rock close to the upper contact to the dolerite seems to be partly fractured, which is mainly indicated by decreased resistivity and partly decreased P-wave velocity. Apart from the dolerite, the geophysical logs indicate mainly low fracture frequency along KLX20A. However, in the section c 410–418 m there is a possible deformation zone indicated by decreased bulk resistivity, partly decreased P-wave velocity, decreased density and decreased magnetic susceptibility.

The estimated porosity shows a fairly constant level of c 0.4–0.5%, apart for the section that intersects the dolerite, along which the estimated apparent porosity is c 0.8–2.0% (Figure 5-6). The porosity is also increased in the section c 411–418 m, which coincides with a possible deformation zone. The estimated salinity is fairly constant at c 240–260 ppm NaCl along the section c 100–158 m. At c 158 m, just above the point where the boreholes reaches the dolerite, the salinity levels starts to increase. At c 235 m, just below the dolerite, the increase stops, and is kept fairly constant at c 1,000 ppm NaCl along the remaining part of the borehole. This indicates that the increased fracturing of the dolerite has an influence on the salinity content of the borehole fluid, possibly related to water bearing fractures.

5.3.3 Interpretation of KLX09B

The results of the generalized logging data and fracture estimations of KLX09B are presented in Figure 5-7 and the distribution of silicate density classes along the borehole is presented in Table 5-4.

The upper half of KLX09B, section c 10–59 m, is characterized by silicate density of 2,680–2,730 kg/m³ and magnetic susceptibility of 0.020–0.040 SI, and the section c 59–100 m (lower half) is dominated by silicate density < 2,680 kg/m³ and magnetic susceptibility in the range 0.010–0.020 SI. The natural gamma radiation shows only minor variations within the range 18–25 µR/h along the borehole, without any clear correlation to the density or susceptibility logs. The data suggest that the rocks along the borehole are dominated by Ävrö granite, with granodioritic composition in the upper half and granitic composition in the lower half.

Mafic dykes (most likely fine-grained diorite/gabbro), indicated by increased density, decreased natural gamma radiation and decreased magnetic susceptibility, occur in the sections c 12.0–14.5 m, 46.0–47.0 m, 49.8–50.5 m and 86.3–86.8 m.

The occurrence of fine-grained granite dykes, which is mainly indicated by increased natural gamma radiation, is suggested at c 35.9–36.3 m, 55.0–55.7 m, 63.1–63.9 m, 67.0–68.0 m, 75.7–76.9 m, 91.3–91.6 m and 95.6–96.0 m.

The estimated fracture frequency is mainly low or moderate. However, two possible deformation zones are indicated in the sections c 48–50 m and 74–80. The sections are characterized by decreased resistivity, decreased magnetic susceptibility and partly decreased P-wave velocity. The upper possible deformation zone coincides with an indicated mafic dyke and the lower possible deformation zone coincides with an indicated fine-grained granite dyke.

Table 5-4. Distribution of silicate density classes with borehole length of KLX09B.

Silicate density interval (kg/m ³)	Borehole length (m)	Relative borehole length (%)
dens < 2,680	26	30
2,680 < dens < 2,730	49	56
2,730 < dens < 2,800	9	10
2,800 < dens < 2,890	2	2
dens > 2,890	2	2

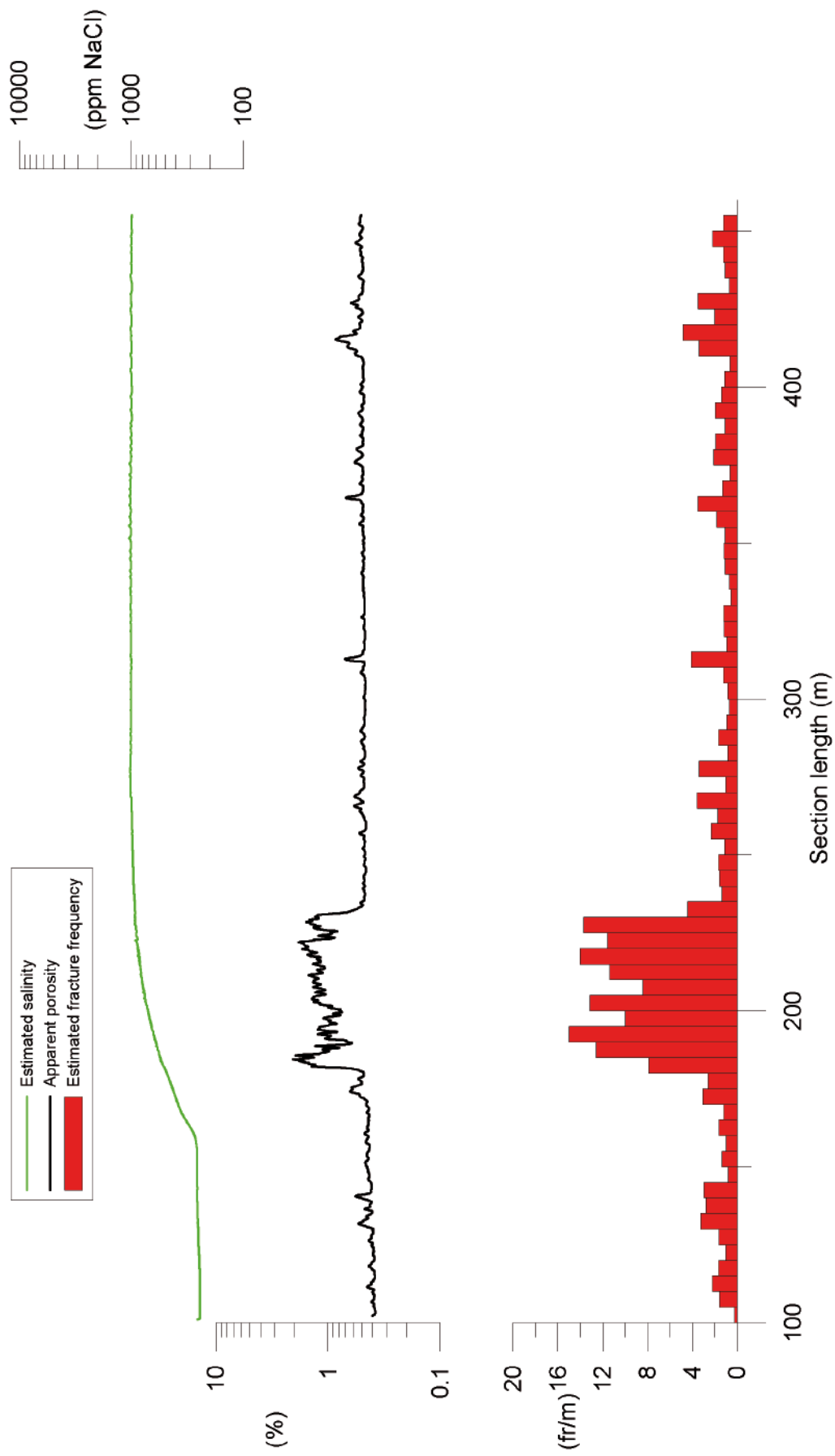


Figure 5-6. Estimated salinity, apparent porosity and estimated fracture frequency of KLX20A.

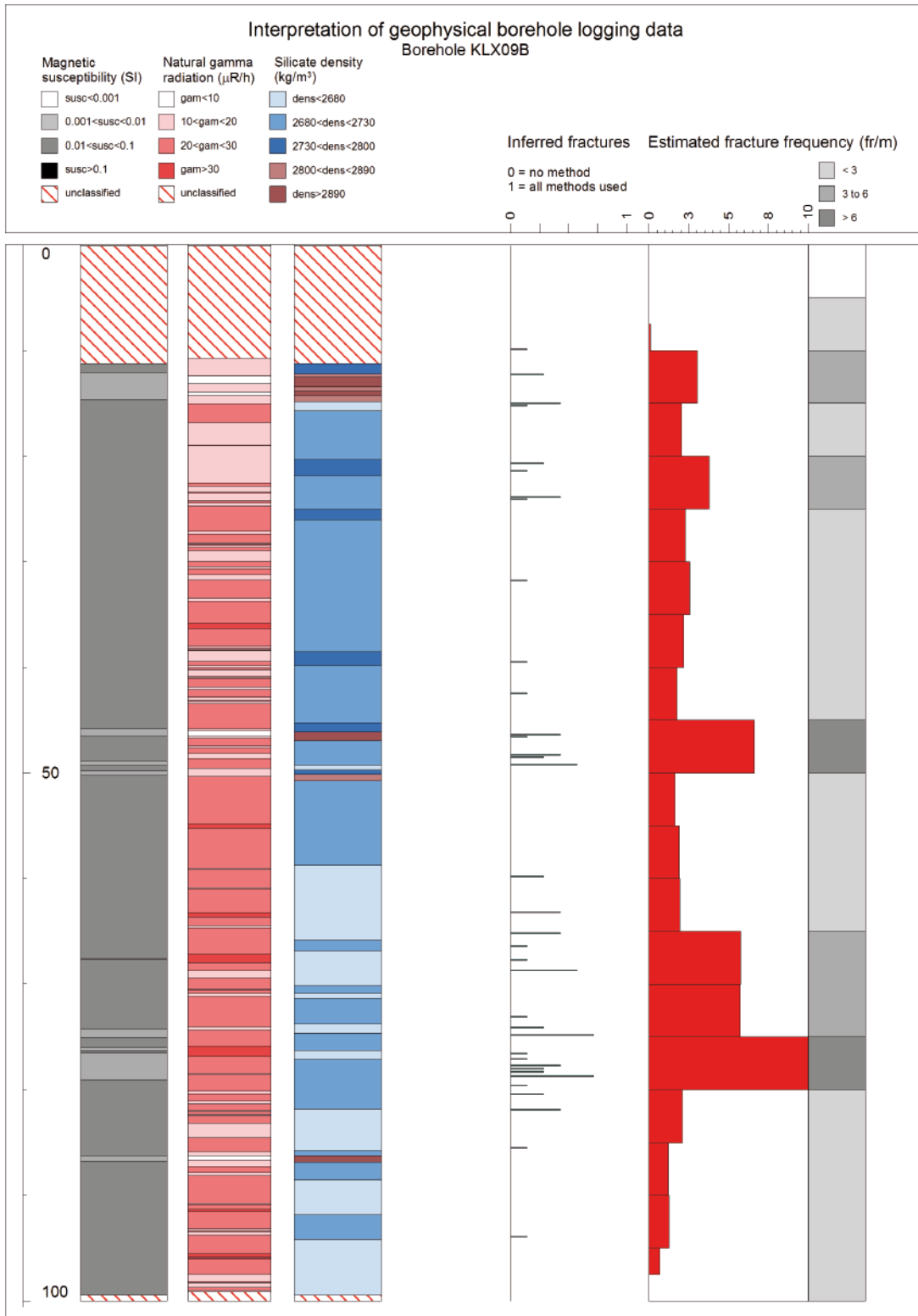


Figure 5-7. Generalized geophysical logs of KLX09B.

The estimated apparent porosity (Figure 5-8) averages at c 0.5%, which is considered normal for crystalline rocks in this area. Increased porosity is clearly related to increased fracturing, and occurs mainly in the section c 73–79 m. The estimated fluid water salinity is fairly constant at c 165–175 ppm NaCl. At c 83 m there is a stepwise increase up to c 214 pp NaCl, which is possibly related to the indicated deformation zone at c 74–80 m.

5.3.4 Interpretation of KLX09D

The results of the generalized logging data and fracture estimations of KLX09D are presented in Figure 5-9 and the distribution of silicate density classes along the borehole is presented in Table 5-5.

The rocks in the vicinity of KLX09D are dominated by silicate density in the intervals $< 2,680 \text{ kg/m}^3$ and $2,680\text{--}2,730 \text{ kg/m}^3$ (the lower density class mainly occurs in the lower half of the borehole). In the corresponding sections the natural gamma radiation is mainly in the interval $15\text{--}25 \text{ } \mu\text{R/h}$ and the magnetic susceptibility averages at c 0.025 SI. The data suggest a dominant occurrence of Ävrö granite with mainly granodioritic composition in the upper half and granitic composition in the lower half of KLX09D.

In the section c 37–58 there is a large occurrence of strong positive anomalies in the natural gamma radiation data, which suggests the occurrence of several fine-grained granite dykes. However, fine-grained granite is usually associated with a strong decrease in the magnetic susceptibility, and this is not the case for some of the sections with increased radiation level, which indicates that the anomalies may be caused by other rock types.

Along the section c 10–30 m there is an increased occurrence of rocks with increased density, in the intervals $2,730\text{--}2,800 \text{ kg/m}^3$, $2,800\text{--}2,890 \text{ kg/m}^3$ and also $> 2,890 \text{ kg/m}^3$. The highest density intervals coincide with decreased magnetic susceptibility and decreased natural gamma radiation, which suggest that fine-grained diorite/gabbro causes these anomalies.

The estimated fracture frequency is mainly low or moderate. Increased fracturing, possible deformation zones, are mainly indicated in the section c 64–71 m and 79–90 m. The upper section is characterized by several short low resistivity anomalies in combination with partly decreased P-wave velocity and partly decreased magnetic susceptibility. The lower section (79–90 m) is characterized by a major decrease in the bulk resistivity, partly decreased P-wave velocity and partly decreased magnetic susceptibility.

The estimated apparent porosity level is in the range 0.4–0.8%, which is slightly increased with respect to what is expected for crystalline rocks (Figure 5-10). The high porosity anomalies, mainly indicated in the interval c 80–90 m, clearly coincide with possible deformation zones

The estimated salinity is fairly constant in the range c 100–120 ppm NaCl in the section c 10–95 m. At c 95 m there is a stepwise increase up to c 220 ppm NaCl, and at c 116.5 m there is a second stepwise increase up c 430 ppm NaCl.

Table 5-5. Distribution of silicate density classes with borehole length of KLX09D.

Silicate density interval (kg/m^3)	Borehole length (m)	Relative borehole length (%)
dens $< 2,680$	35	32
$2,680 < \text{dens} < 2,730$	60	55
$2,730 < \text{dens} < 2,800$	10	10
$2,800 < \text{dens} < 2,890$	2	2
dens $> 2,890$	1	1

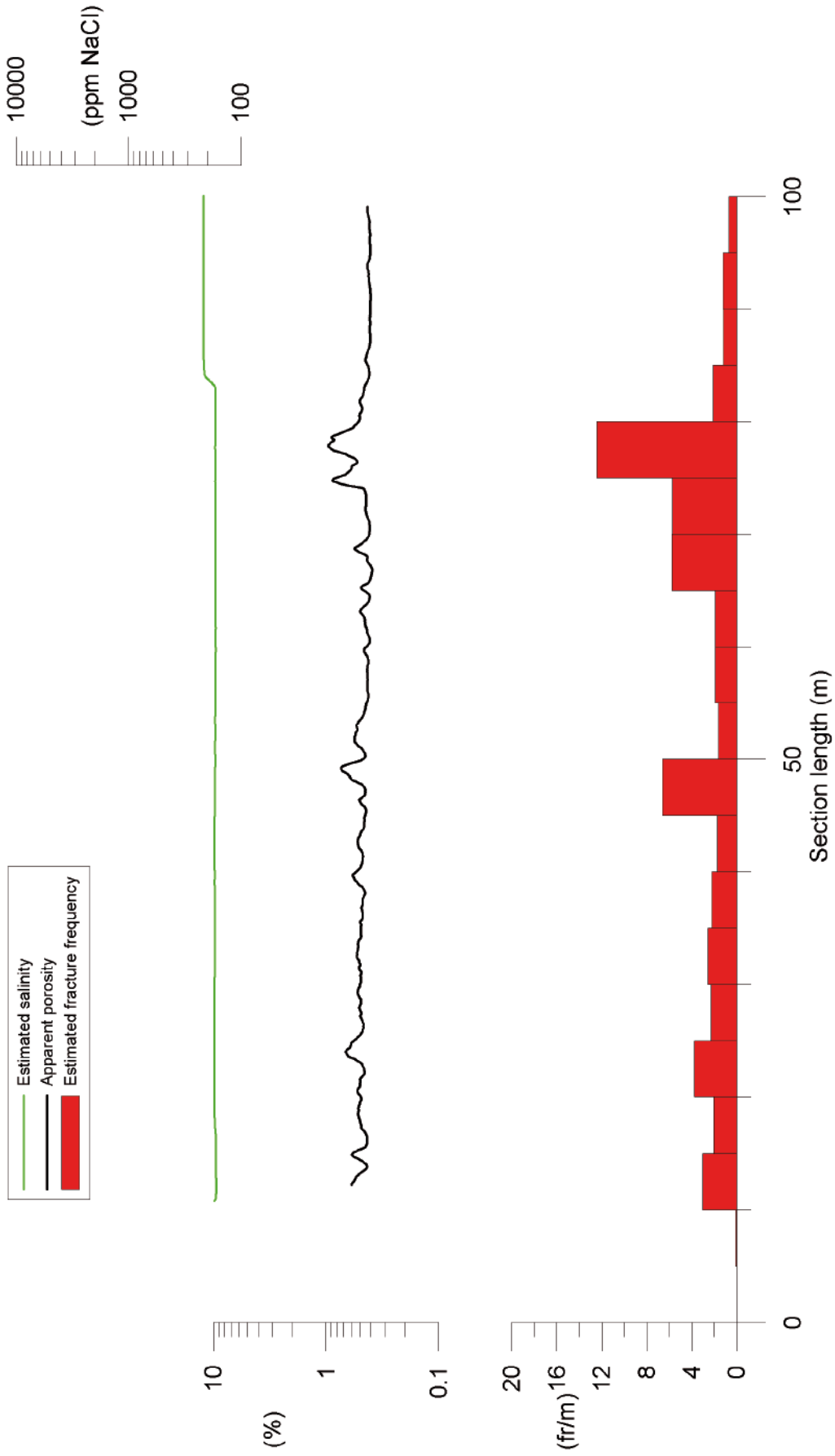


Figure 5-8. Estimated salinity, apparent porosity and estimated fracture frequency of KLX09B.

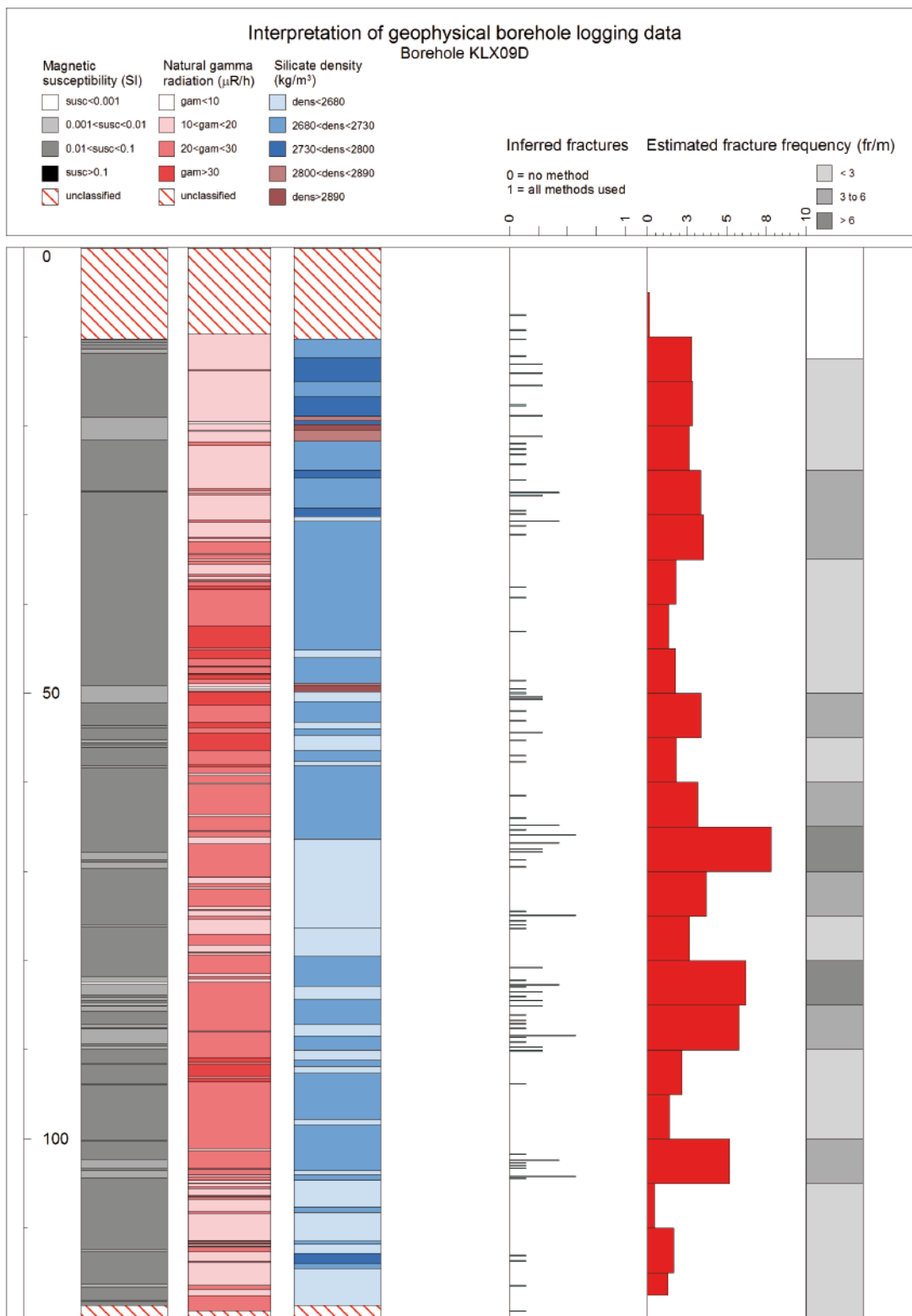


Figure 5-9. Generalized geophysical logs of KLX09D.

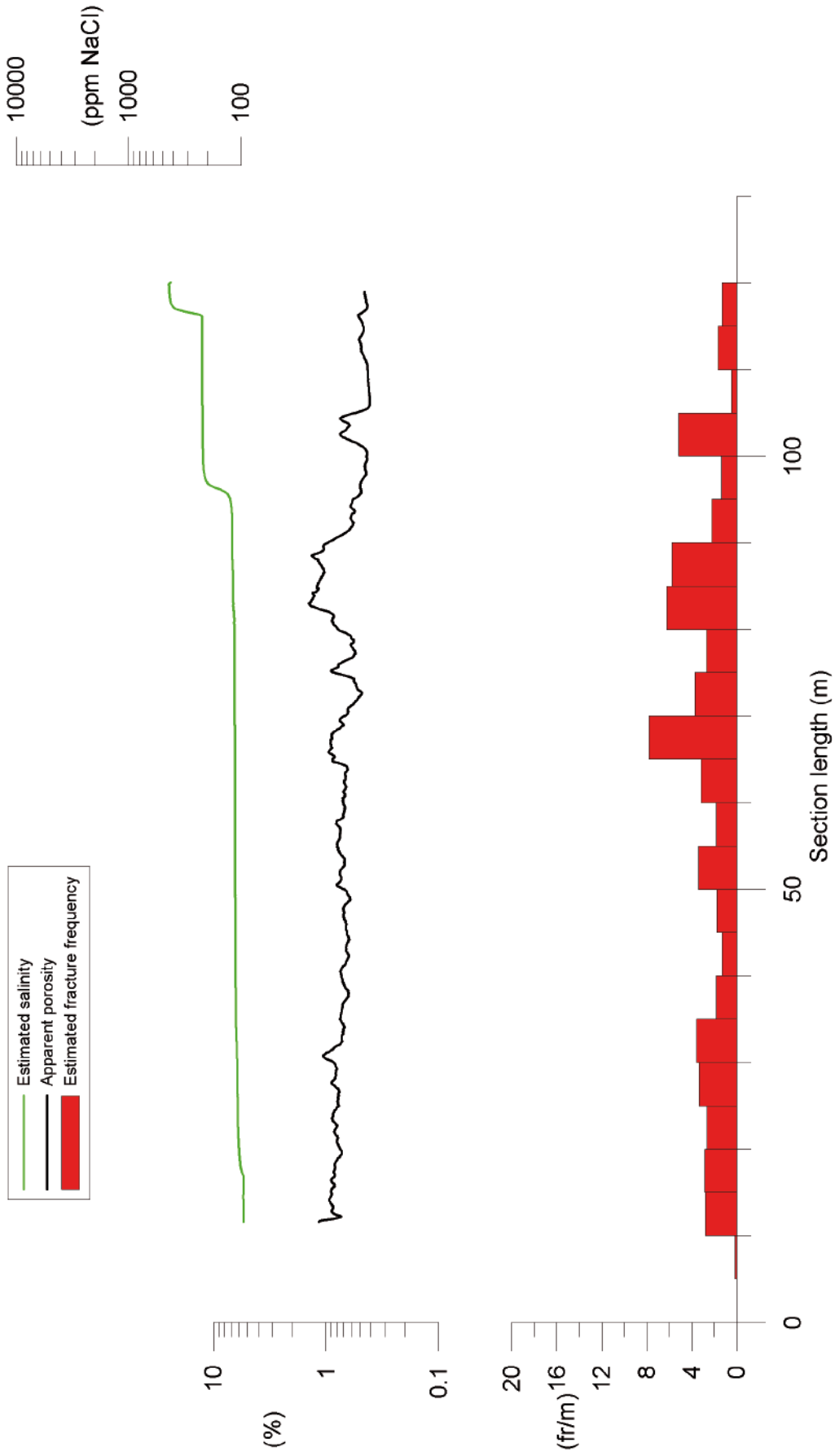


Figure 5-10. Estimated salinity, apparent porosity and estimated fracture frequency of KLLX09D.

5.3.5 Interpretation of KLX09F

The results of the generalized logging data and fracture estimations of KLX09F are presented in Figure 5-11 and the distribution of silicate density classes along the borehole is presented in Table 5-6.

The silicate density log shows that the rocks in the vicinity of KLX09F mainly have silicate density $< 2,680 \text{ kg/m}^3$, but there is also a fair occurrence of rocks with silicate density in the range $2,680\text{--}2,730 \text{ kg/m}^3$. The natural gamma radiation is generally in the range $c 20\text{--}30 \text{ } \mu\text{R/h}$ and the magnetic susceptibility is in the range $0.015\text{--}0.035 \text{ SI}$. The rocks along the borehole are most likely dominated by Ävrö granite with a granitic mineral composition. In the section $c 10\text{--}85 \text{ m}$ there is relatively larger occurrence of sections with decreased magnetic susceptibility as compared to the lower half of the borehole.

There is a strong positive radiation anomaly in the section $c 37\text{--}47 \text{ m}$, which coincides with decreased density and decreased magnetic susceptibility. The combination of physical properties is typical for fine-grained granite. Minor occurrences of mafic rock (most likely fine-grained diorite/gabbro) are indicated in the sections $c 48\text{--}51 \text{ m}$ and $105\text{--}106 \text{ m}$.

The estimated fracture frequency is generally low or partly moderate. A possible deformation zone is indicated in the section $c 67\text{--}83 \text{ m}$. The section is characterized by decreased resistivity and decreased magnetic susceptibility and one minor interval with decreased P-wave velocity. This suggests dominant ductile deformation or sealed fractures in combination with mineral alteration.

The estimated apparent porosity is $c 1.3\%$ at the top of the borehole, and shows a constant decrease down to the bottom, ending at a level of $c 0.4\%$ (Figure 5-12). The behavior is clearly correlated to the estimated fluid water salinity log, which shows that the software used for calculating the porosity fails to compensate for the variation in fluid water resistivity. The high porosity level should therefore most likely be ignored. It is however clear that the possible deformation at $c 67\text{--}83 \text{ m}$ zone coincides with increased apparent porosity. The estimated salinity starts at $c 135 \text{ ppm NaCl}$ at the top of the borehole, increases constantly, and ends at $c 215 \text{ ppm NaCl}$. This behavior indicates that the fluid water was not in chemical equilibrium at the time of the logging measurements.

Table 5-6. Distribution of silicate density classes with borehole length of KLX09F.

Silicate density interval (kg/m^3)	Borehole length (m)	Relative borehole length (%)
dens $< 2,680$	82	58
$2,680 < \text{dens} < 2,730$	50	35
$2,730 < \text{dens} < 2,800$	7	5
$2,800 < \text{dens} < 2,890$	3	2
dens $> 2,890$	1	0

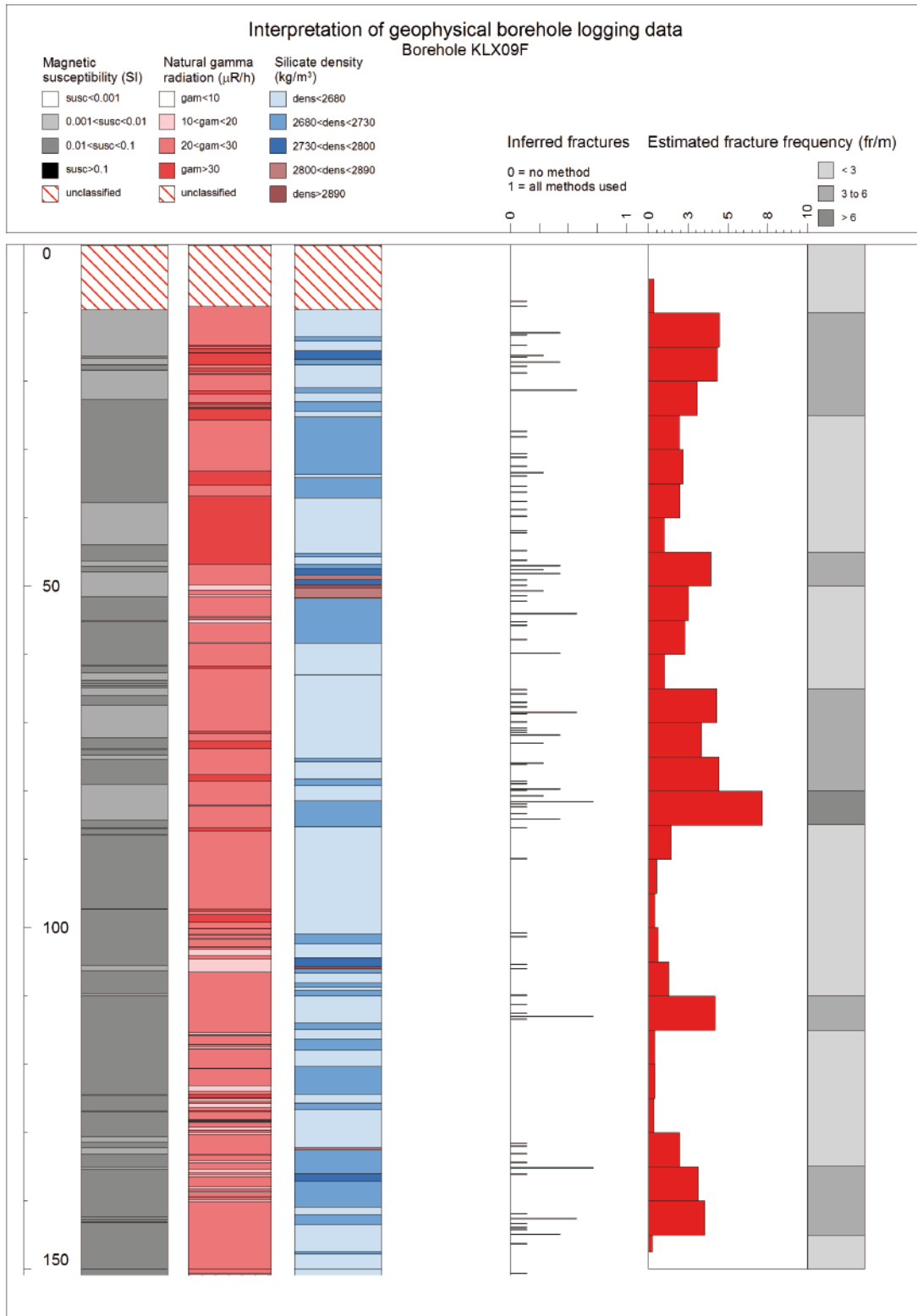


Figure 5-11. Generalized geophysical logs of KLX09F.

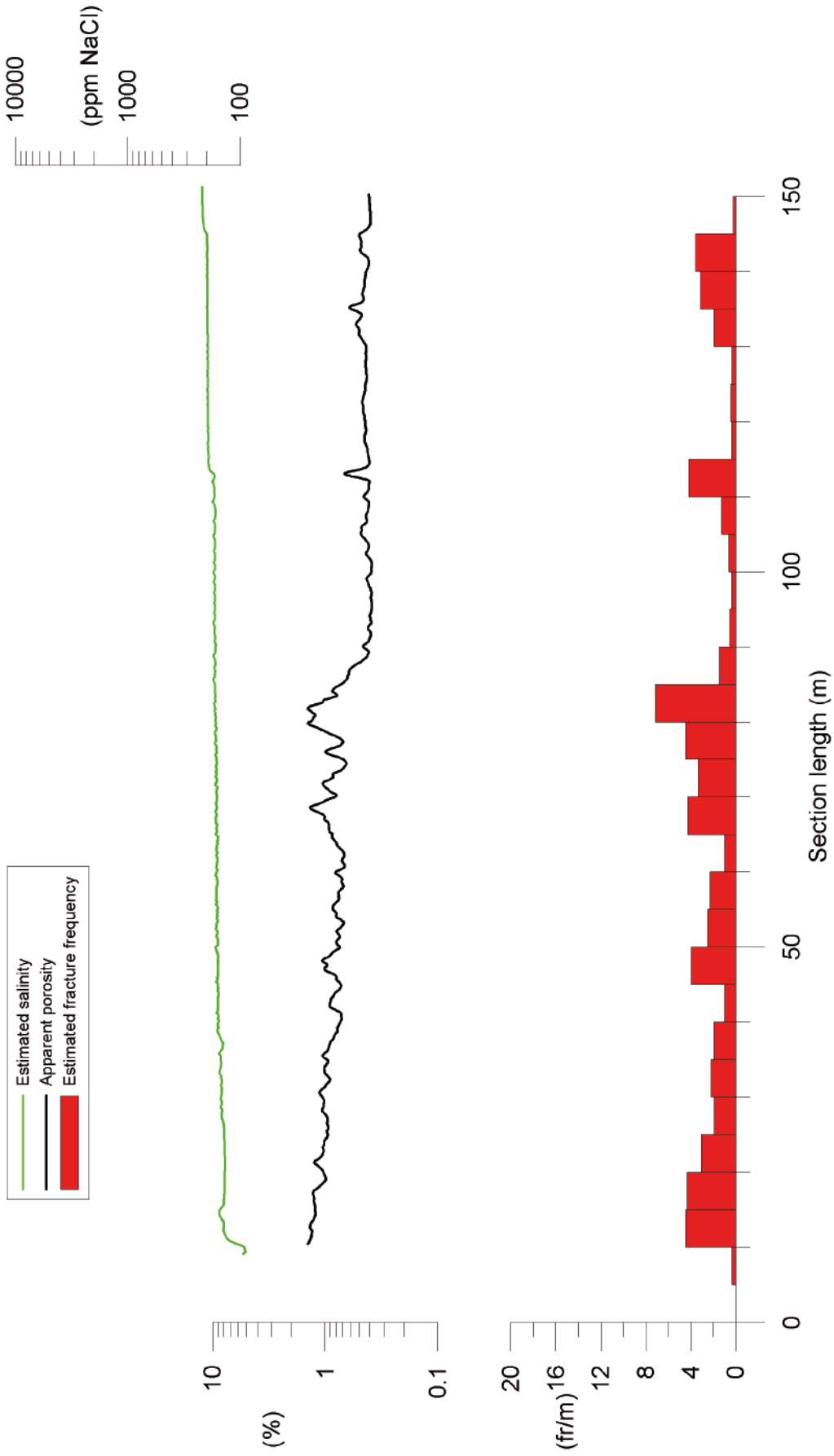


Figure 5-12. Estimated salinity, apparent porosity and estimated fracture frequency of KLX09F.

5.3.6 Interpretation of KLX11B

The results of the generalized logging data and fracture estimations of KLX11B are presented in Figure 5-13 and the distribution of silicate density classes along the borehole is presented in Table 5-7.

The silicate density log shows a complete dominance of rocks with silicate density in the range 2,730–2,780 kg/m³. In the corresponding section the magnetic susceptibility is 0.025–0.030 SI and the natural gamma radiation is mainly in the interval 10–20 µR/h, but partly also in the interval 20–30 µR/h. The combination of physical properties indicates that the rock occurrence in the vicinity of KLX11B is mainly governed by quartz monzodiorite, or possibly Ävrö granite with high content of dark minerals and/or low content of quartz.

Mafic rocks hardly seem to occur at all in KLX11B and there are only few indicated occurrences of fine-grained granite (mainly one at the top and one at the bottom of the borehole).

The estimated fracture frequency of KLX11B is mainly moderate and partly low. Possible deformation zones are indicated in the section c 60–65 m, 75–80 m, and 87–89 m. The uppermost section is characterized by several short low resistivity anomalies in combination with partly decreased P-wave velocity and partly decreased magnetic susceptibility. The section 75–80 m is characterized by a major decrease in the bulk resistivity, partly decreased P-wave velocity and only a minor decrease in the magnetic susceptibility. The lowermost indicated deformation shows a major decrease in the resistivity, in the magnetic susceptibility and also in the density. In the section there is slightly increased natural gamma radiation, possibly indicating the occurrence of felsic rock.

The estimated apparent porosity is fairly constant at the level c 0.4%. Minor anomalies of increased porosity occur in sections with indicated increased fracturing (Figure 5-14). The estimated salinity is almost constant at c 160–170 ppm NaCl. In the lowermost c 25 m of the borehole there is a slight increase in the salinity level, up to c 210 ppm NaCl.

5.3.7 Interpretation of HLX38

The results of the generalized logging data and fracture estimations of HLX38 are presented in Figure 5-15.

In HLX38 no density or caliper data were collected in the section c 64–125 m. The reason for this lack of data is not known. The silicate density log shows a dominance of rocks with silicate density in the range 2,680–2,730 kg/m³ in the vicinity of borehole. There are fair occurrences of sections with silicate density in the range 2,730–2,800 kg/m³ and there are also some intervals with silicate density < 2,680 kg/m³. There are no indications of mafic rocks (diorite/gabbro) in HLX38. The density data most likely indicate a dominant occurrence of Ävrö granite.

The natural gamma radiation averages at c 16 µR/h, which in combination with the silicate density data suggest that the Ävrö granite has low amount of quartz and/or high amount of dark minerals. Short sections with increased natural gamma radiation, most likely related to the occurrences of fine-grained granite dykes, occur abundantly along the entire borehole length.

Table 5-7. Distribution of silicate density classes with borehole length of KLX11B.

Silicate density interval (kg/m ³)	Borehole length (m)	Relative borehole length (%)
dens < 2,680	3	3
2,680 < dens < 2,730	17	18
2,730 < dens < 2,800	75	78
2,800 < dens < 2,890	1	1
dens > 2,890	0	0

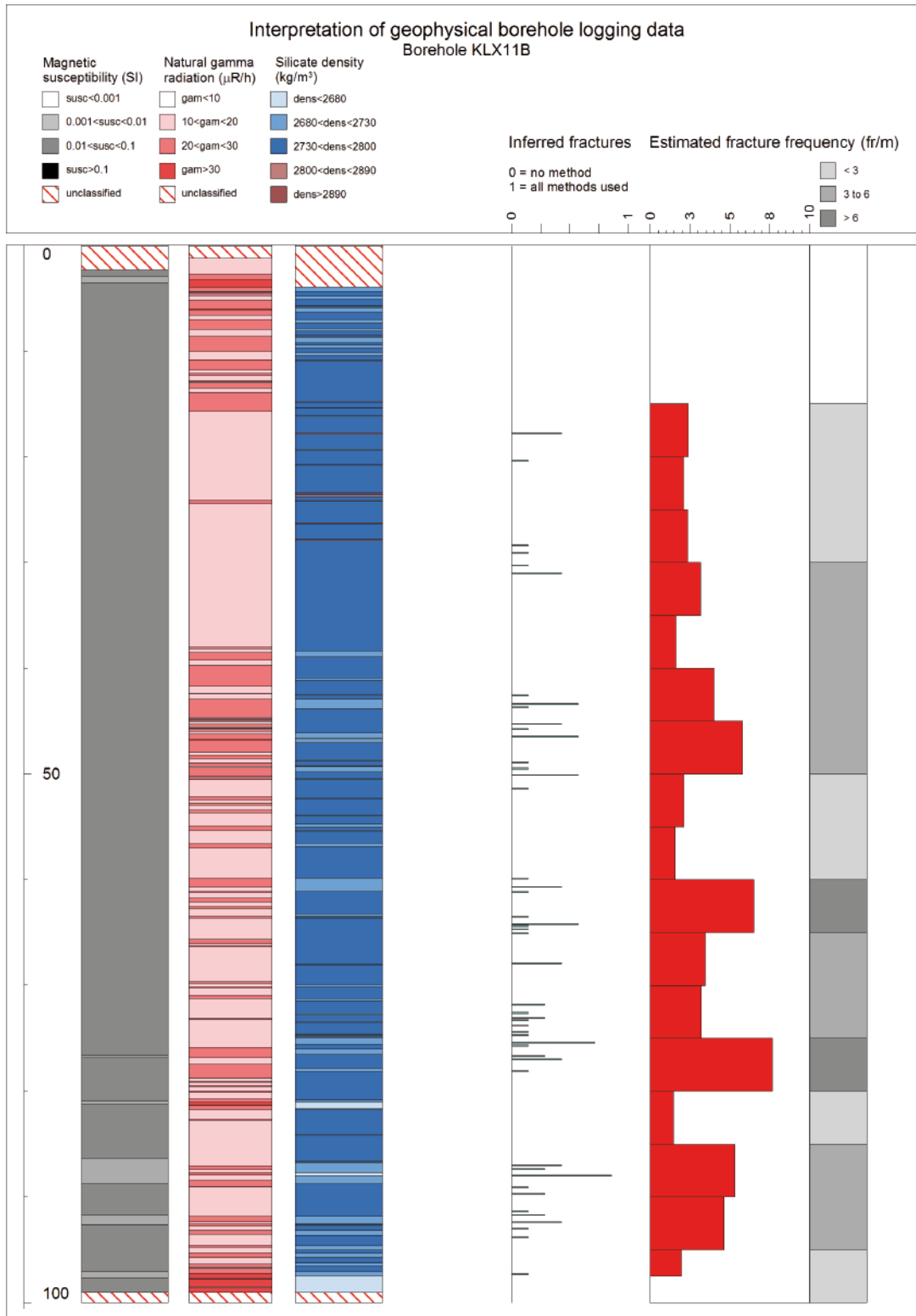


Figure 5-13. Generalized geophysical logs of KLX11B.

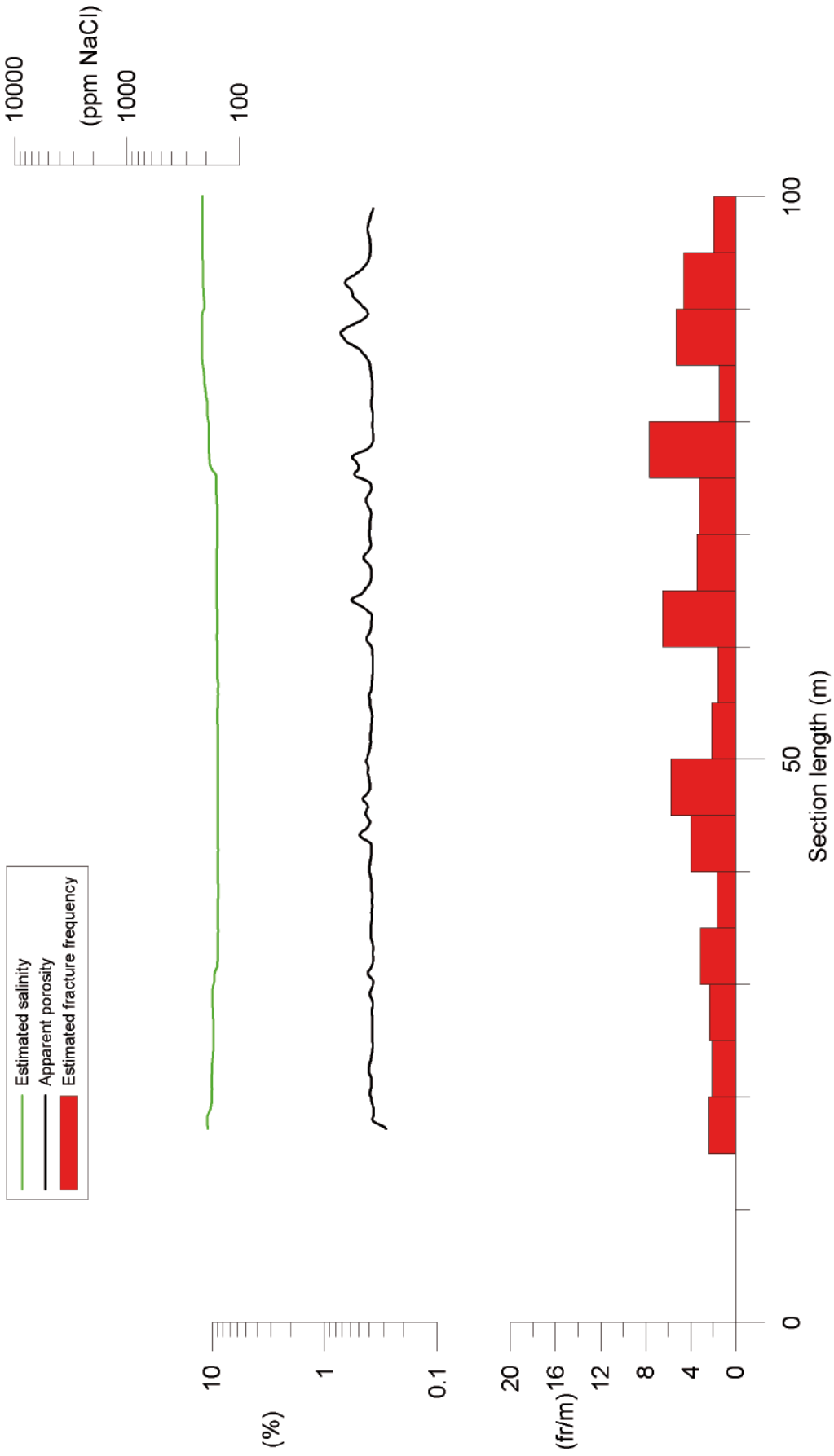


Figure 5-14. Estimated salinity, apparent porosity and estimated fracture frequency of KLX11B.

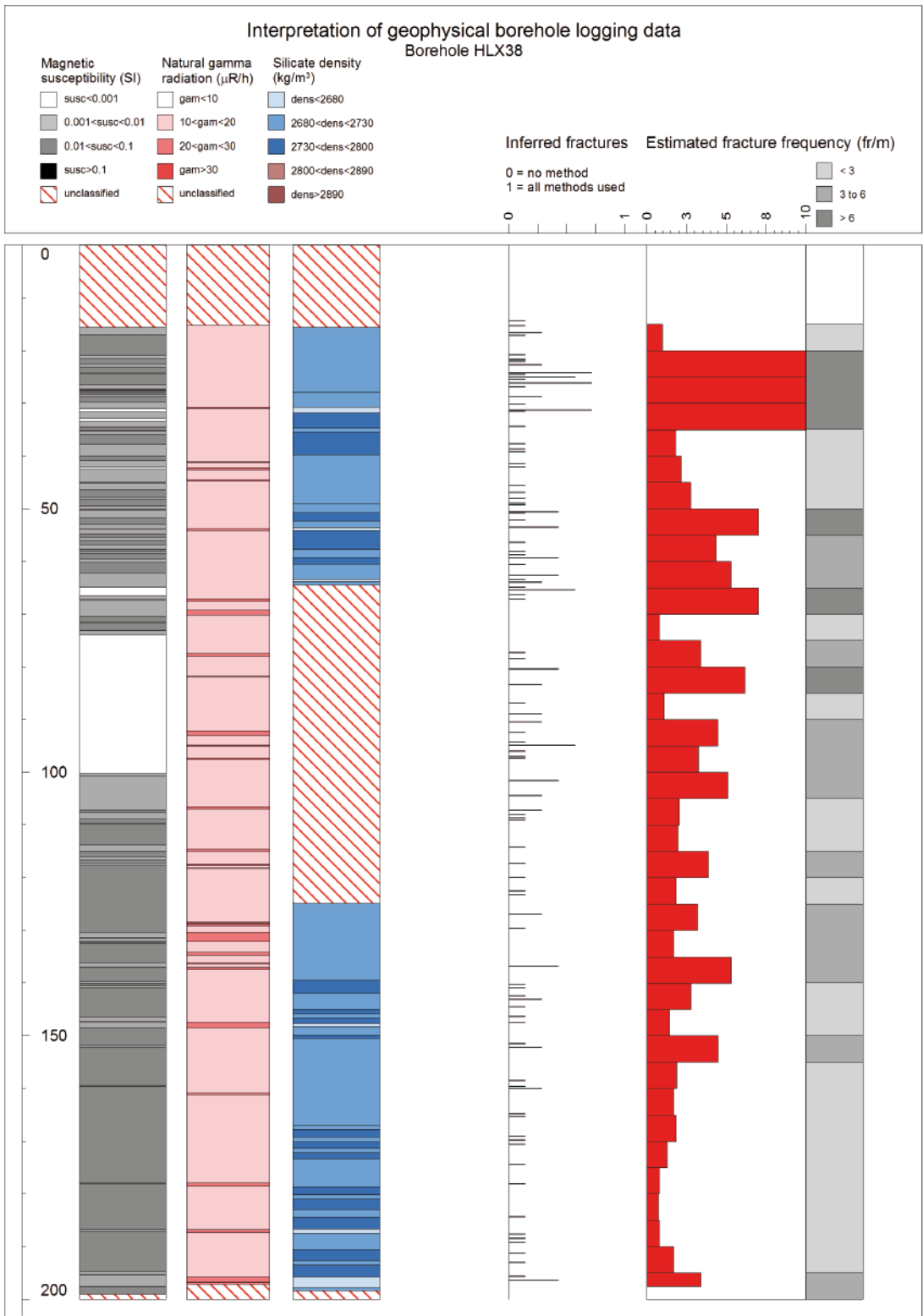


Figure 5-15. Generalized geophysical logs of HLX38.

The magnetic susceptibility is generally in the range c 0.010–0.015 SI, which is low relative to the usual susceptibility level of Ävrö granite of c 0.03–0.05 SI. In the section c 74–101 m there is a major drop in magnetic susceptibility, down to c 0.0003–0.0007 SI, which indicates mineral alteration (often related to deformation) and/or a different rock type. The natural gamma radiation data do not show any anomalous variations in this section compared to the other parts of the borehole. Since there are no density data available the reason for the low susceptibility is difficult to explain. Also, neither the sonic nor the resistivity logs show any significant indications of deformation along the low magnetic section.

The estimated fracture frequency indicates several sections with moderate or high fracturing, though there is a dominance of low fracture frequency. When viewing the individual logs (sonic, resistivity and caliper), it seems that the estimated fracture frequency is exaggerated. Possible deformation zones (based on the primary data) are indicated in the sections c 23–32 m and 62–67 m. The upper section is characterized by decreased resistivity, partly decreased P-wave velocity, partly decreased magnetic susceptibility and a significant caliper anomaly at c 31.5 m. The lower section is characterized by decreased resistivity, significantly decreased magnetic susceptibility and partly decreased P-wave velocity.

5.3.8 Interpretation of HLX39

The results of the generalized logging data and fracture estimations of HLX39 are presented in Figure 5-16.

The silicate density log shows a dominance of rocks with silicate density in the range 2,680–2,730 kg/m³ in the vicinity of borehole. There are also some intervals with silicate density < 2,680 kg/m³, the longest in the start and at the end of the borehole. In the section c 29.5–31.0 m, 87.8–88.5 m, 166.0–167.0 m and 178.0–181.0 the density is greater than 2,820 kg/m³. All these sections coincide with increased magnetic susceptibility, which indicates that the rock type is diorite/gabbro (not fine-grained).

In the section c 6–83 m the magnetic susceptibility averages at c 0.015 SI and in the lower half of the borehole, section c 83–200 m the average susceptibility is c 0.030 SI. In the intervals c 75–83 m and c 190–200 m there is a major decrease in the magnetisation.

The natural gamma radiation is fairly constant in the interval 10–20 µR/h. Decreased natural gamma radiation generally coincide with increased density. Short sections (< 1.0 m) with increased natural gamma radiation are concentrated in the interval c 60–160 m. Many of these most likely correspond to fine-grained granite dykes.

The fracture frequency estimated for HLX39 is mainly low and partly moderate. Possible deformation zones are indicated in the sections c 13–17 m (decreased resistivity, decreased magnetic susceptibility and caliper anomaly), c 75–83 m (major decrease in bulk resistivity, decreased magnetic susceptibility, caliper anomalies and minor decrease in P-wave velocity) and c 190–192 m (decreased resistivity, minor decrease in P-wave velocity, caliper anomaly and decreased magnetic susceptibility).

5.3.9 Interpretation of HLX40

The results of the generalized logging data and fracture estimations of HLX40 are presented in Figure 5-17.

The silicate density varies greatly between the two classes < 2,680 kg/m³ and 2,680–2,730 kg/m³. The average wet density is c 2,700 kg/m³, with only minor variations, which shows that the large variations indicated in Figure 5-17 are mainly caused by the fact that the density varies up and down across the boundary between two classes. The natural gamma radiation log data are almost constant along the borehole, with an average of 8±2 µR/h, which is anomalously low if the rock type is Ävrö granite.

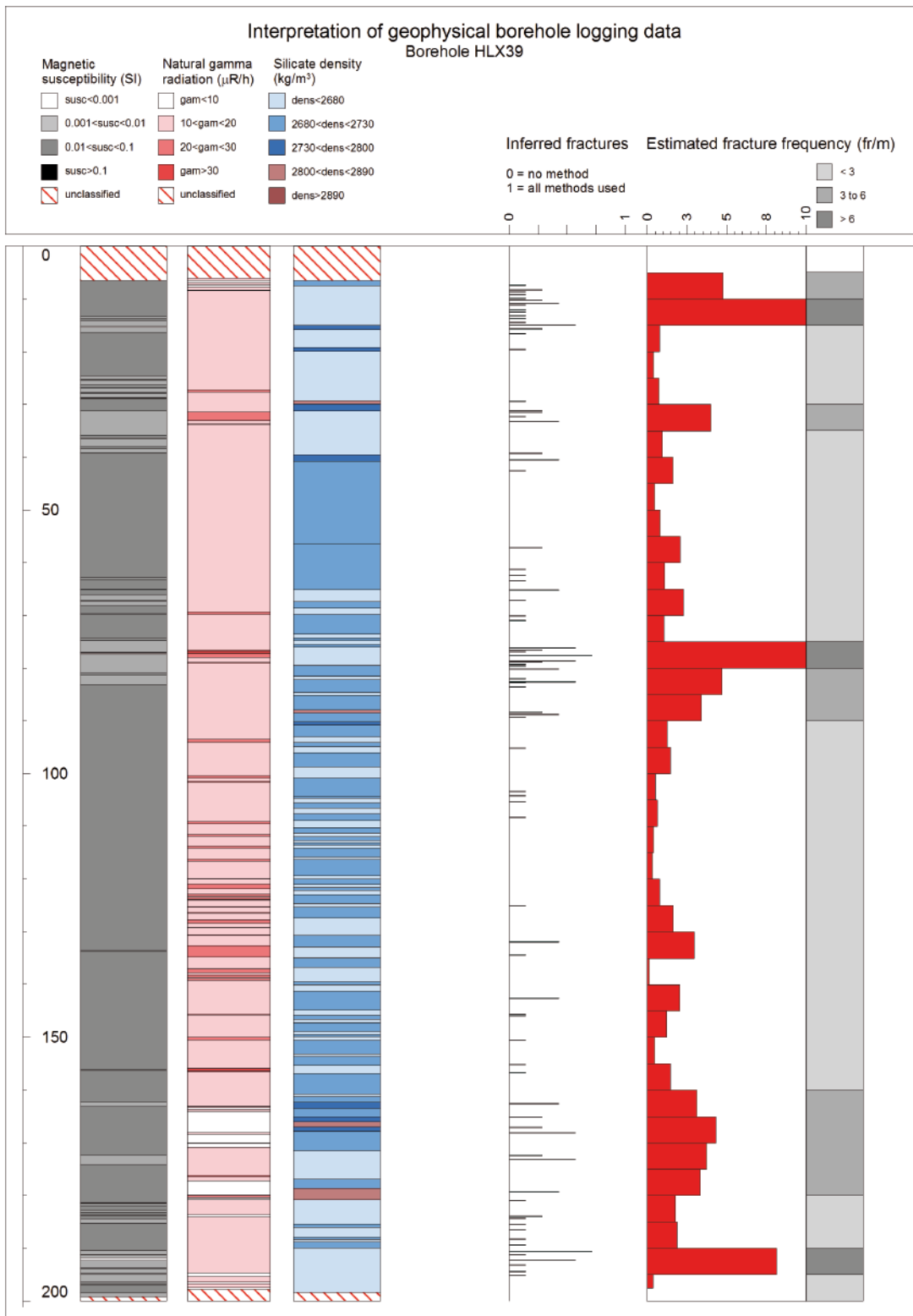


Figure 5-16. Generalized geophysical logs of HLX39.

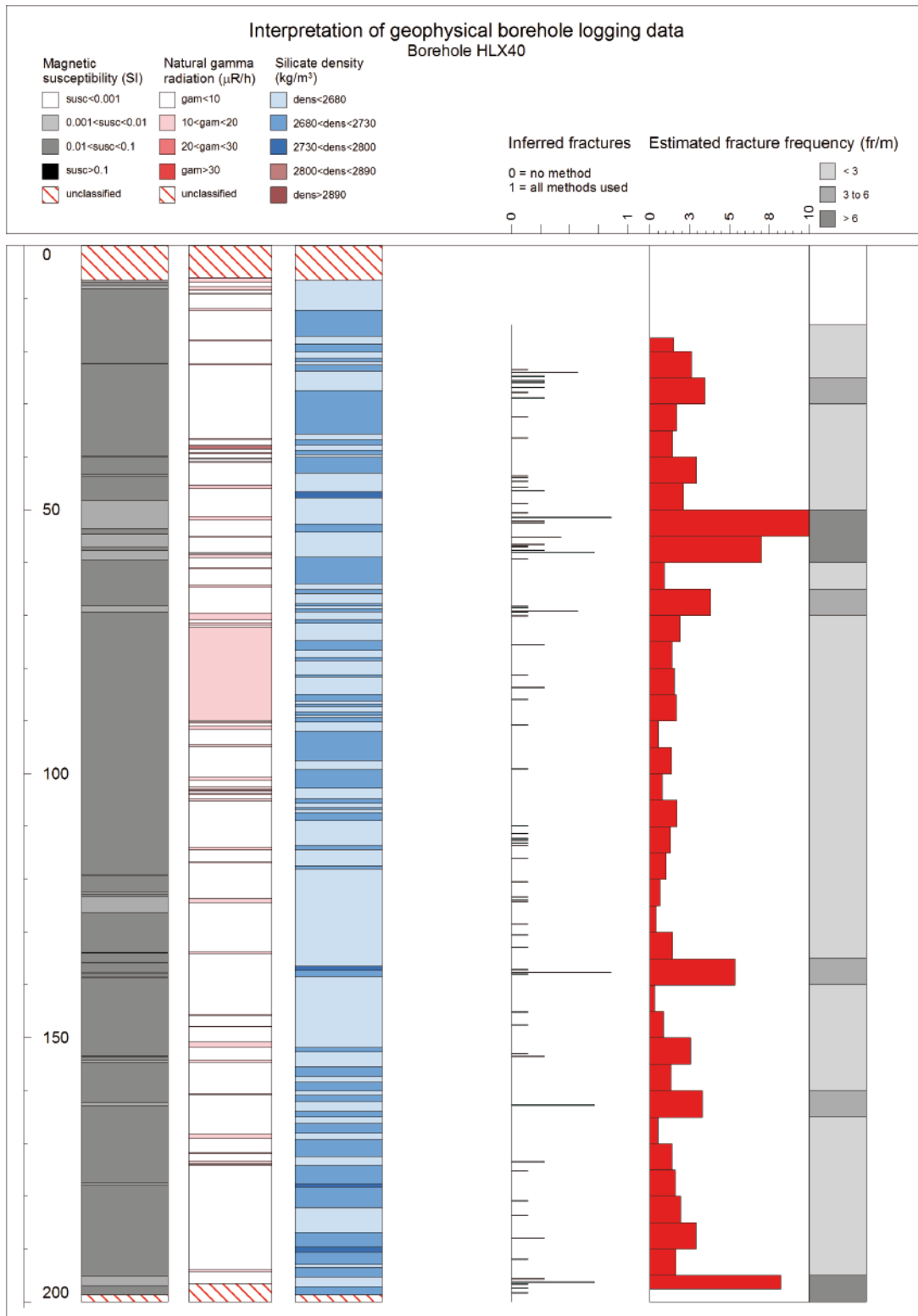


Figure 5-17. Generalized geophysical logs of HLX40.

The magnetic susceptibility is mainly in the range 0.015–0.030 SI, with three magnetic lows occurring in the intervals c 48–59 m, 123–126 m and 192–197 m.

The combination physical properties in HLX40 indicate a complete dominance of Ävrö granite along the entire borehole.

In the section c 120–150 m there is a distinct decrease in density (2,640 kg/m³) and magnetic susceptibility (0.017 SI), which indicates a possible change in rock type or, perhaps more likely, compositional variations in the Ävrö granite. There are no significant changes in the natural gamma radiation along this interval.

The estimated fracture frequency is mainly low. Two possible deformation zones are indicated in the intervals c 50–60 m and 192–197 m. Both sections are characterized by decrease magnetic susceptibility, decreased resistivity, decreased P-wave velocity and caliper anomalies.

5.3.10 Interpretation of HLX41

The results of the generalized logging data and fracture estimations of HLX41 are presented in Figure 5-18.

A large part of HLX41, section c 5–144 m is totally dominated by rocks with silicate density < 2,680 kg/m³. Section c 144–200 m shows a dominance of silicate density in the range 2,680–2,730 kg/m³. However, when looking at the density log data (primary log data after calibration) the wet density log reveals more information and shows a complex distribution. The sections c 5–33 m, 70–90 m and 100–140 m show fairly constant density of 2,660 kg/m³. The sections c 33–57 m and 165–200 m also show rather constant density of c 2,700 kg/m³. There are also three low density sections at c 57–70 m, 90–100 m and 155–160 m with an average density of c 2,610 kg/m³.

In the section c 146–150 m there is a significant increase in the density, in combination with increased magnetic susceptibility and decreased natural gamma radiation, which suggests the occurrence of diorite/gabbro.

The natural gamma radiation is fairly constant along the entire borehole, with an average of c 14 µR/h. Three strong positive radiation anomalies occur close to the bottom of the borehole. The anomalies most likely correspond to fine-grained granite dykes.

The magnetic susceptibility is fairly constant in the range c 0.020–0.030 SI. Three significant magnetic lows occur in the section c 57–70 m, c 90–100 m and c 153–160. Observe the almost perfect correlation with low density sections.

The fracture frequency of HLX41 is generally low. A possible major deformation zone is indicated in the fracture frequency plots in Figure 5-18 along the section c 5–40 m. However, this is most likely a false indication caused by a major drop in fluid water resistivity at c 40 m. Above the drop the resistivity logs show large variations and below the drop the resistivity log hardly show and anomalies at all. The reason for this is that when the fluid water resistivity becomes very low the major part of the current from the transmitter electrode fails to reach out in the rock volume, the measured potential difference becomes small and the resistivity method does not work well. When looking at the sonic and caliper data it is fairly clear that there are no major deformation zones in HLX41. Minor deformation zone are indicated in the sections c 156–160 m and 192–195 m; characterized by decreased resistivity and decreased P-wave velocity.

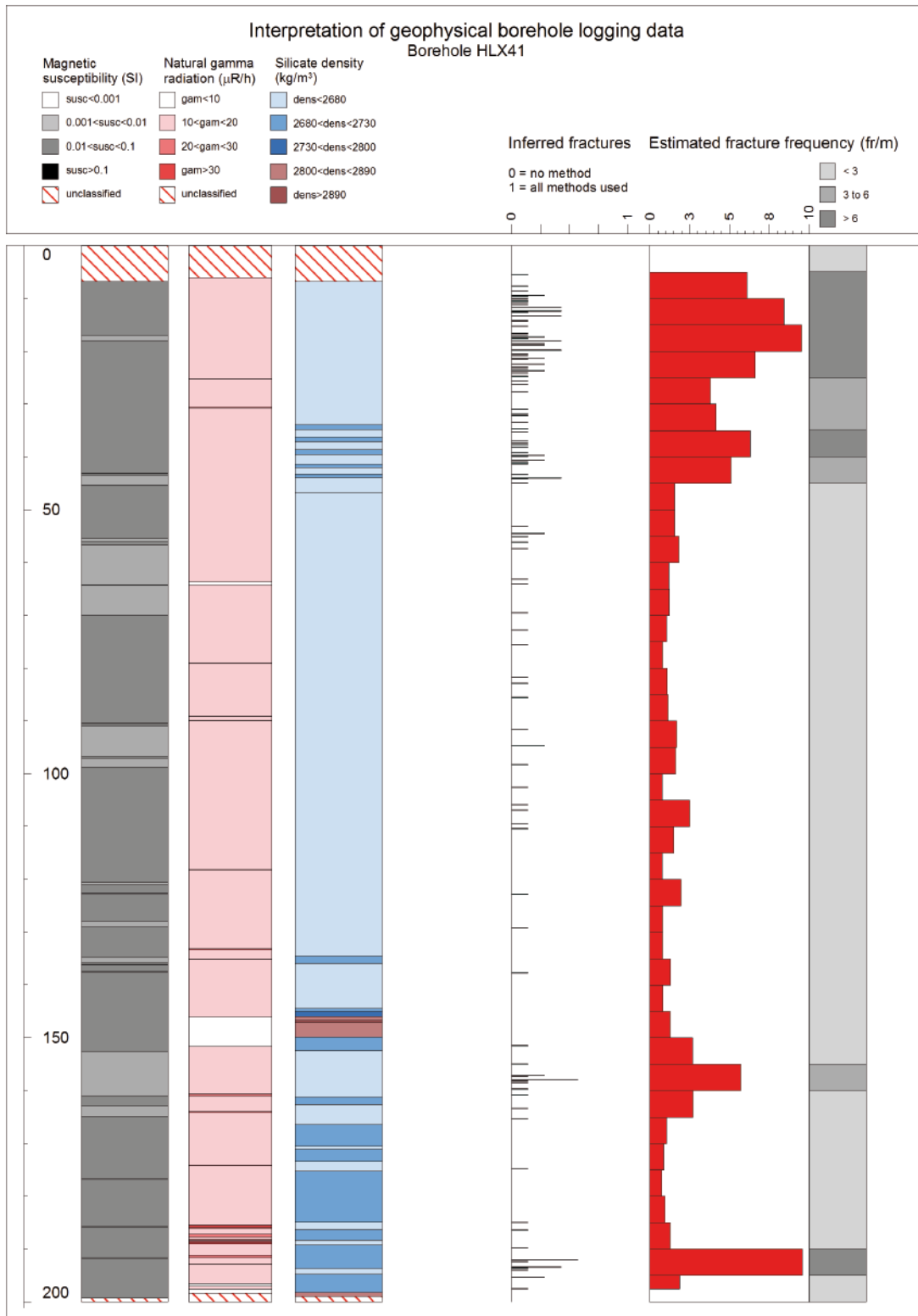
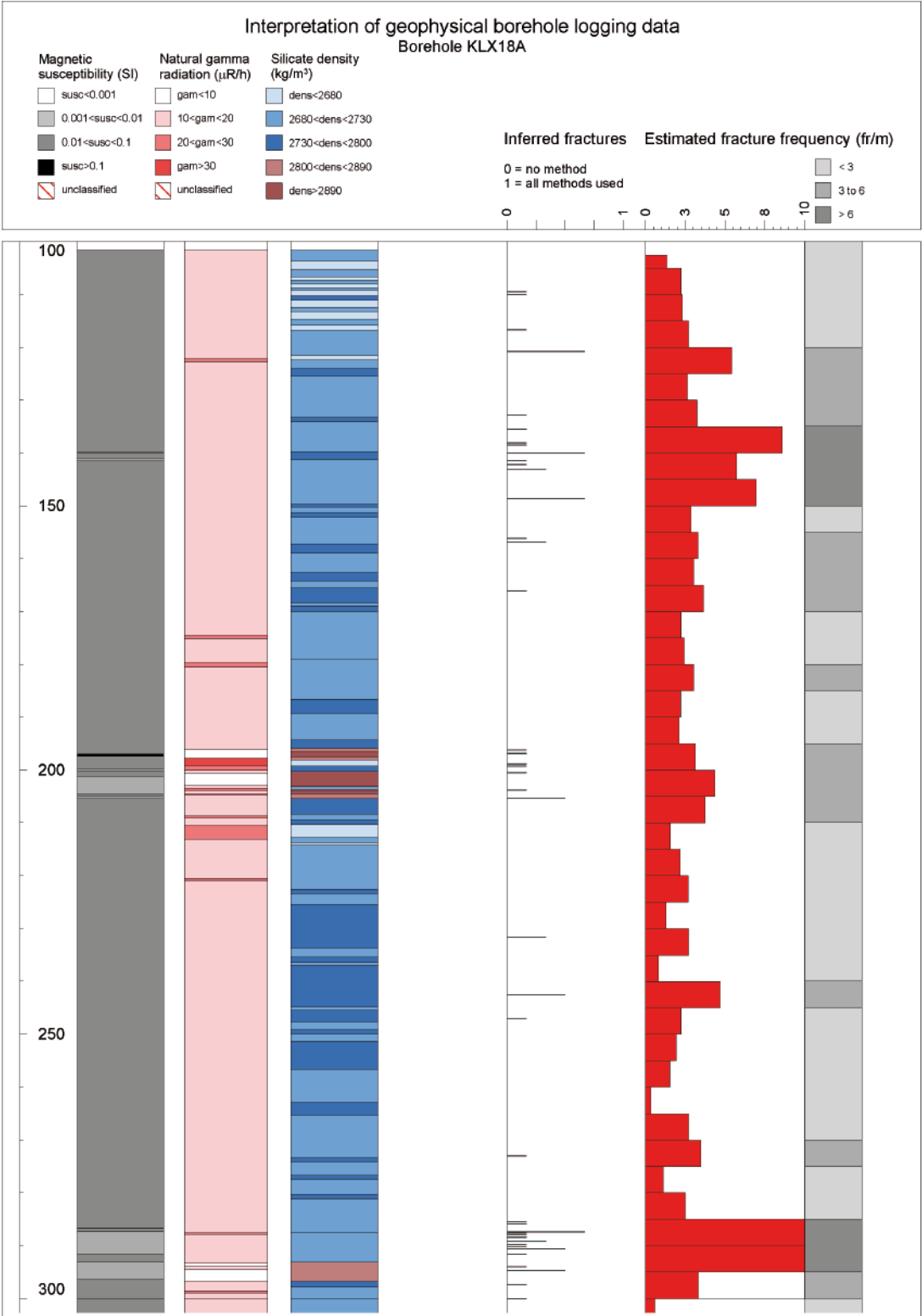


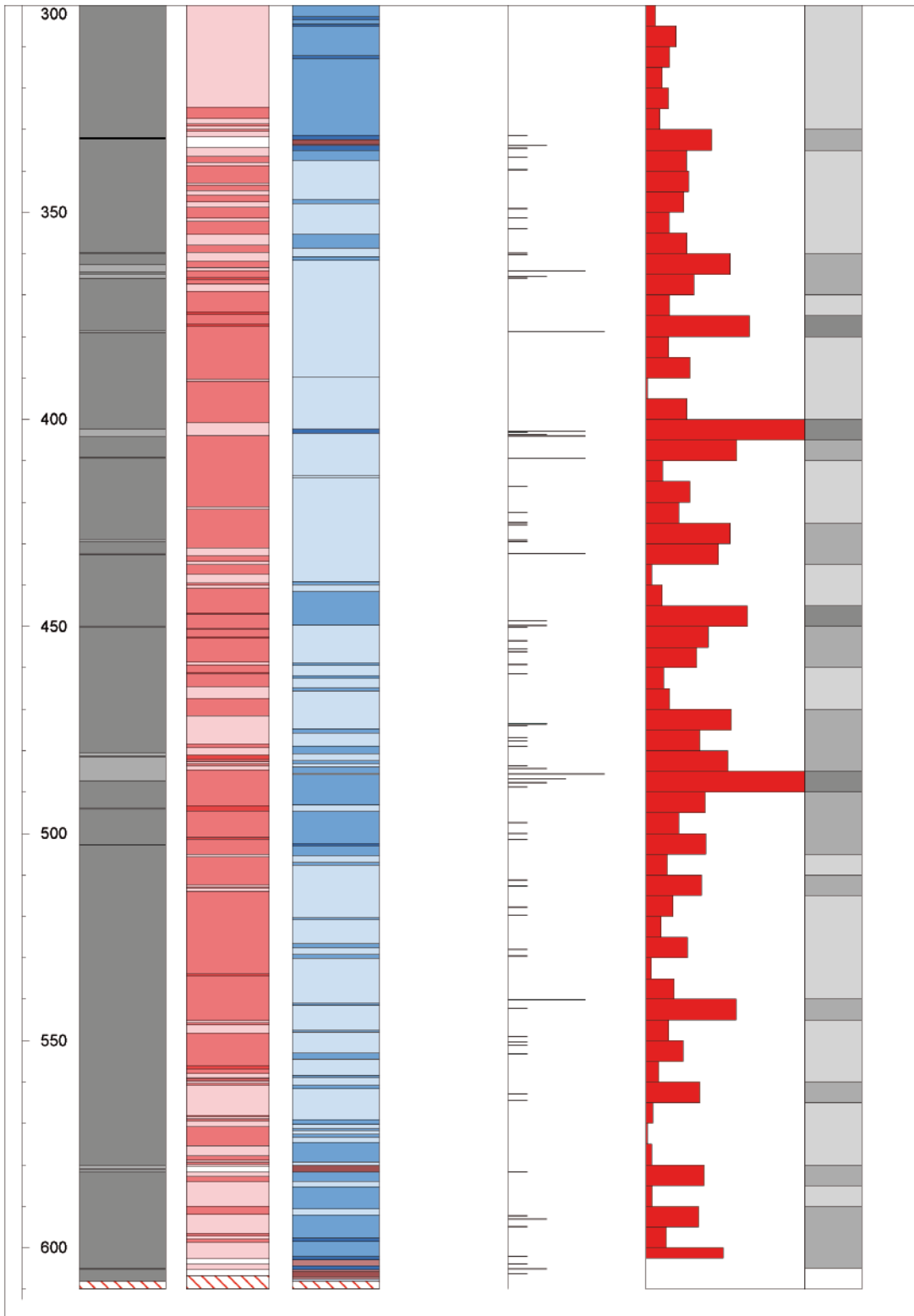
Figure 5-18. Generalized geophysical logs of HLX41.

References

- /1/ **Nielsen U T, Ringgaard J, 2006.** Geophysical borehole logging in boreholes KLX20A, KLX18A, KLX11B, KLX09B, KLX09D, KLX09F, HLX38, HLX39, HLX40 and HLX41. SKB P-06-290, Svensk Kärnbränslehantering AB. In Press.
- /2/ **Mattsson H, Thunehed H, Keisu, M, 2005.** Interpretation of geophysical borehole measurements and compilation of petrophysical data from KLX01, KLX03, KLX04, HLX21, HLX22, HLX23, HLX24, HLX25, HLX26, HLX27 and HLX28. SKB P-05-34, Svensk Kärnbränslehantering AB.
- /3/ **Mattsson H, Thunehed H, 2004.** Interpretation of geophysical borehole data from KSH01A, KSH01B, KSH02 (0–100m), HSH01, HSH02 and HSH03, and compilation of petrophysical data from KSH01A and KSH01B. SKB P-04-28, Svensk Kärnbränslehantering AB.
- /4/ **Mattsson H, Thunehed H, 2004.** Interpretation of geophysical borehole data and compilation of petrophysical data from KSH02 (80–1,000m) and KAV01. SKB P-04-77, Svensk Kärnbränslehantering AB.
- /5/ **Mattsson H, 2004.** Interpretation of geophysical borehole data and compilation of petrophysical data from KSH03A (100–1,000m), KSH03B, HAV09, HAV10 and KLX02 (200–1,000m). SKB P-04-214, Svensk Kärnbränslehantering AB.
- /6/ **Mattsson H, 2004.** Interpretation of geophysical borehole data and compilation of petrophysical data from KAV04A (100–1,000m), KAV04B, HLX13 and HLX14. SKB P-04-217, Svensk Kärnbränslehantering AB.
- /7/ **Mattsson H, 2006.** Interpretation of geophysical borehole measurements and petrophysical data from KLX10. SKB P-06-162, Svensk Kärnbränslehantering AB.
- /8/ **Keisu M, 2006.** Calibration of 1D and 3D caliper data from core and percussion drilled boreholes. SKB P-06-153, Svensk Kärnbränslehantering AB.
- /9/ **Henkel H, 1991.** Petrophysical properties (density and magnetization) of rock from the northern part of the Baltic Shield. *Tectonophysics* 192, 1 – 19.
- /10/ **Puranen R, 1989.** Susceptibilities, iron and magnetite content of precambrian rocks in Finland. Geological survey of Finland, Report of investigations 90, 45 pp.
- /11/ **Archie G E, 1942.** The electrical resistivity log as an aid in determining some reservoir characteristics: *Trans. Am. Inst. Min., Metallurg., Petr.Eng.*, 146, 54–62.

Generalized geophysical logs of KLX18A





Generalized geophysical logs of KLX20A

